UNIVERSITY OF CALIFORNIA, SAN DIEGO

A RabGAP Protein and BEACH Family Proteins Regulate Contractile Vacuole Formation and Activity and Chemotaxis in *Dictyostelium*

A dissertation submitted in partial satisfaction of the requirements for the degree of Doctor of Philosophy

in

Biology

by

Fei Du

Committee in charge:

Professor Richard A. Firtel, Chair
Professor Joan H. Brown
Professor Scott D. Emr
Professor Randy Hampton
Professor Steven A. Wasserman

2007

The dissertation of Fei Du is approved, and it is acceptable in quality and in form for publication on microfilm:

Chair

University of California, San Diego

2007

DEDICATION

To my parents Xueming Du and Shunjiao Xiao,

and my husband, Feng Xu,

without whose love and support,

none of this would have ever been possible.

TABLE OF CONTENTS

LIST OF SYMBOLS

RabGAP	Rab GTPase Activity Protein
ER	Endoplasmic Reticulum
CV	Contractile Vacuole
EM	Electron Microscopy
NBD-Cl	7-chloro-4-nitrobenzo-2-oxa-1,3-diazole
V-ATPase	Vacuolar-Proton ATPase
CHS	Chediak-Higashi Syndrome
BEACH	Beige and CHS
LYST	Lysosomal Trafficking Regulator
Lvs	Large Volume of Sphere
Arp2/3	Actin-Related Protein 2/3
InsP(3)	Inositol 1,4,5-trisphosphate

LIST OF FIGURES

Chapter I

Chapter II

LIST OF TABLES

Chapter II

ACKNOWLEDGEMENTS

I would like to thank Dr. Richard A. Firtel and Dr. Scott D. Emr for their mentorship towards the production of this dissertation. I would like to give thanks to the other members of my thesis committee, Dr. Joan H. Brown, Dr. Randy Hampton, and Dr. Steve A. Wasserman, for their expert guidance and time.

I would like to acknowledge all members of the Firtel laboratory for their scientific discussions and suggestions. I especially thank Susan Lee, who taught me many of the techniques used in the lab and whose friendship helped me through the five years of studies. I would like thank Jennifer Roth for help in preparing my manuscripts.

The text of Chapter I, in part, is material to be submitted for publication in 2007, by Fei Du, Kimberly Edwards, Zhouxin Shen, Binggang Sun, Steven Briggs, Arturo De Lozanne, and Richard A. Firtel. Co-author Richard A. Firtel guided and supervised the writing of the introductory material.

Chapter II, in part, is material to be submitted for publication in 2007, by Fei Du, Kimberly Edwards, Zhouxin Shen, Binggang Sun, Steven Briggs, Arturo De Lozanne, and Richard A. Firtel. The dissertation author was the primary investigator and author of this paper. Co-author Kimberly Edwards performed REMI suppressor/enhancer screening with me and did co-immunoprecipitation of RabGAP1. Zhouxin Shen and Steven Briggs performed mass spectrometry analysis of the RabGAP1 complex. Binggang Sun did yeast two-hybrid screening using ERK1 as bait and identified the *rabgap1* gene. Arturo De

Lozanne provided the LvsA knock-in, *drainin*$^{-}$ cell line and the anti-LvsA antibody. Co-author Richard A. Firtel supervised the work, in whole.

VITA

1998 B.S. Wuhan University

2001 M.S. Cancer Institute, Peking Union Medical University & Chinese Academy of Medical Sciences

2007 Ph.D. University of California, San Diego

PUBLICATIONS

Fei Du, Kimberly Edwards, Zhouxin Shen, Binggang Sun, Steven Briggs, Arturo De Lozanne, Richard A. Firtel. 2007. Regulation of Contractile Vacuole Formation and Activity in *Dictyostelium* by Two TBC-domain Containing Proteins and BEACH Family Proteins. Submitted to Developmental Cell.

Michelle C. Mendoza, Fei Du, Negin Iranfar, Nan Tang, Hui Ma, William F. Loomis, and Richard A. Firtel. 2005. Loss of SMEK, a Novel, Conserved Protein, Suppresses *mek1* Null Cell Polarity, Chemotaxis, and Gene Expression Defects. Molecular and Cellular Biology, 25(17): 7839-7853

ABSTRACT OF THE DISSERTATION

A RabGAP Protein and BEACH Family Proteins Regulate Contractile Vacuole Formation and Activity and Chemotaxis in *Dictyostelium*

by

Fei Du

Doctor of Philosophy in Biology

University of California, San Diego, 2007

Professor Richard A. Firtel, Chair

The contractile vacuole (CV) system is the osmoregulatory organelle of free-living amoebae and protozoa. I present data showing that the RabGAP RabGAP1 acts as a switch for discharging the CVs into the extracellular medium in *Dictyostelium*. *rabgap1* null (*rabgap1*$^-$) cells have highly enlarged CVs whose structure and activity are aberrant. In *rabgap1*$^-$ cells, the dynamic fusion of the CV with the plasma membrane is

absent and the discharge of CV content is inefficient. RabGAP1 localizes to the CV membrane whereupon the vacuoles stop charging, become round, and fuse to the plasma membrane. Drainin, another TBC-domain containing protein, and RabGAP1 sequentially localize to the CV membrane and regulate CV discharge. Rab8A and Rab11A interact with RabGAP1, co-localize with RabGAP1 on the CV, and suppress the *rabgap1*$^{-}$ large vacuole phenotype. However, Rab8A suppresses both the large vacuole phenotype and the abnormal discharging phenotype in *drainin*$^{-}$ cells. I identified two BEACH family proteins, LvsA and LvsD, as a suppressor and an enhancer of the *rabgap1*$^{-}$ large CV phenotype, respectively. Analysis of LvsA and LvsD mutant strains in a *rabgap1*$^{-}$ background revealed that LvsA and LvsD have distinct functions in regulating CV biogenesis by controlling the recycling of CV membranes. My studies help define the pathways controlling CV regulation and biogenesis.

In the last part of the dissertation, I provide evidence that CVs might be the intracellular storage of Ca^{2+} to regulate F-actin polymerization and chemotaxis in *Dictyostelium*.

Chapter I

Introduction

Dictyostelium as a Model System

In this dissertation, I use *Dictyostelium discoideum* to investigate the functions of RabGAPs and BEACH family proteins. *Dictyostelium* is a powerful system in which to study cytokinesis, motility, phagocytosis, chemotaxis, signal transduction, and aspects of development such as cell sorting, pattern formation, and cell-type determination because many of these cellular behaviors and biochemical mechanisms are either absent or less accessible in other model organisms.

In nature, *Dictyostelium* cells live in the soil and feed on bacteria. They can sense folic acid, which is released by bacteria, a natural food source, and chemotax towards their prey, whereupon the bacteria are engulfed by phagocytosis. Once they consume all the nutrients, *Dictyostelium* cells initiate a developmental pathway that results in the formation of a multicellular organism. Approximately 4 hours after starvation, cells begin to release cAMP and chemotax into multicellular aggregation centers, and later differentiate into fruiting bodies composed of vacuolated stalk cells and spore cells (Figure 1). In the laboratory, simply by removing nutrients, one can cause the wild-type cells to start this developmental program. Up to 100,000 cells signal each other by releasing the chemoattractant cAMP and aggregate together by chemotaxis to form a mound that is similar to the type observed in nature. Many of the underlying molecular and cellular processes have remained fundamentally unchanged throughout evolution, which makes *Dictyostelium* a good model system in which to study chemotaxis and

development.

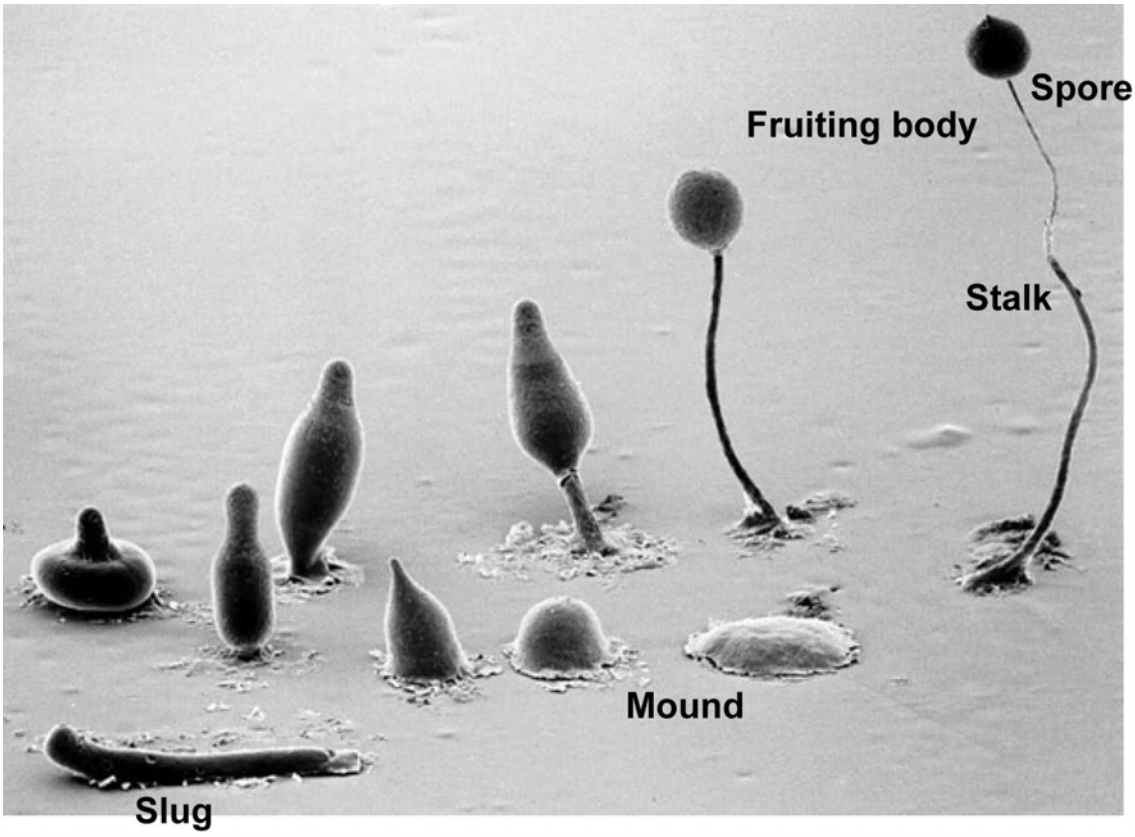

Figure 1:
Development of *Dictyostelium discoideum*. Upon starvation, *Dictyostelium* cells initiate a developmental pathway that results in the formation of a multicellular organism. Up to 100,000 cells signal each other by releasing the chemoattractant cAMP and aggregate together by chemotaxis to form a mound. After around 24 hours, they differentiate into fruiting bodies composed of vacuolated stalk cells and spore cells. The image is adapted from *Dictybase*. Copyright, M.J. Grimson & R.L. Blanton.

The advantage of *Dictyostelium* in the study is that the organism is more amenable to genetic and biochemical analyses than metazoans. A proteome-based phylogeny shows that the amoeba diverged from the animal-fungal lineage after the plant-animal split. Genetically, the amoebae retain more of the diversity of the original

ancestor genome than animals, fungi, or plants [1]. The whole genome of *D. discoideum* has been sequenced, which facilitates identifying, cloning, and characterizing new genes [1]. *D. discoideum* has 6 chromosomes and its genome is about 34 Mb encoding 12,500 ORFs (open reading frames) [1]. *Dictyostelium* exists as a haploid which makes it easy to produce knockout strains and introduce exogenous genes. A variety of autotrophic and dominant drug selectable markers (G418, uracil, thymidine, blasticidin, bleomycin, and hygromycin) together with Cre-loxP system allow one to construct double, triple, or even sextuple gene knockout strains [2]. The genetic tools available in *Dictyostelium* include conventional mutagenesis, gene disruption, antisense, gene replacement, and REMI [3], which can be used for primary and second-site mutagenesis screens.

Breakthroughs for eukaryotic cells have been made from the studies of *Dictyostelium* such as the discoveries: conventional myosin is required for cytokinesis [4]; chemoattractants are sensed by G-protein-coupled receptors [5, 6]; PI3K and PTEN work as an antagonistic pair to control PI(3,4,5)P_3 levels to mediate cell movement, polarity, and chemotaxis [7-9]; and protein ubiquitination pathways are involved in differentiation and pattern formation [10].

The CV System in *Dictyostelium*

In addition to the endoplasmic reticulum (ER) and the Golgi apparatus, *Dictyostelium* cells have two major vesicle systems, the endosomal system and the CV

system. Both systems share some proteins on their membranes, such as vacuolar H^+-ATPase (V-ATPase) and Rab14 [11, 12], suggesting the fusion or the same origin of the membranes of both systems. Endosomal pathways regulate the uptake of nutrients by phagocytosis or macropinocytosis and the secretion or transport of proteins to the cell surface by exocytosis [13]. The CV complex serves as an osmoregulatory organelle that allows cells to survive under hypotonic stress in free-living amoebae and protozoa. It controls intracellular water balance by accumulating and expelling excess water out of the cell membrane. In *Dictyostelium*, the CV system consists of tubules and vacuoles (also called bladders; Figure 2) which are interconvertible [14, 15]. The tubular structures function as collecting ducts to accumulate excess water and fill the bladders with water. The bladders fuse with the plasma membrane to expel water from the cell body [16]. It is suggested that the CV does not disappear during the discharge stage. Instead, the CV collapses, flattens, and maintains its distinct membrane components from the plasma membrane, and the discharge of CV is suggested to be a "kiss and run" event [17]. Electron microscopy (EM) images show that the CV membrane is unique, with packed proton pumps and devoid of actin filaments (Figure 2), whereas the plasma membrane is coated with actin filaments and lacks proton pumps [17]. The components of the liquid that CV systems pump out is still unknown, but it is supposed to be hypotonic to function as an osmoregulatory organelle under hypotonic osmotic stress [18]. The Gerisch group has identified an integral membrane protein named Dajumin which localizes specifically

to the CV system, but not to endosomes or lysosomes [19]. Dajumin localizes to the bladder structures of CV system as well as to the tubular structures [19]. No phenotype is associated with overexpression of Dajumin. Thus, a fluorescent protein fusion of Dajumin serves as a specific CV marker.

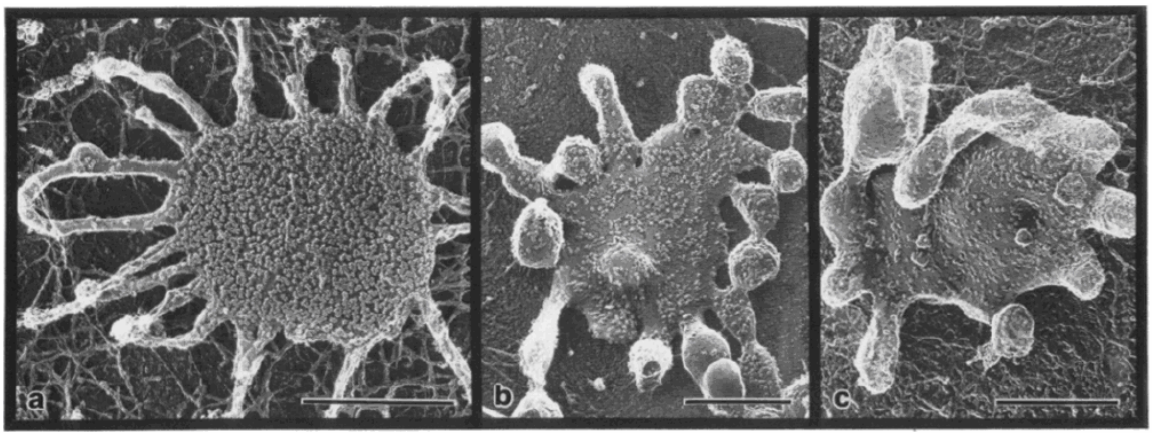

Figure 2:
Three examples of EM images of freeze-dried, broken *Dictyostelium* cells. All represent the intermediate stage in the charging and discharging cycle of the CV. The membrane pegs are vacuolar-proton pumps. The image is from paper [16] Figure 8.

Sesaki and colleagues have found that the CV system also offers an unconventional transport pathway to secrete proteins to the cell surface [20]. DdCAD-1 is a Ca^{2+}-dependent cell-cell adhesion molecule lacking a hydrophobic signal peptide or a transmembrane domain. DdCAD-1 localizes inside of the lumen of the CV as well as the cell surface. The accumulation of DdCAD-1 is greatly reduced under hyper-osmotic conditions and increased after hypotonic treatments. Treatment with NBD-Cl (7-chloro-4-nitrobenzo-2-oxa-1,3-diazole), a CV activity inhibitor, leads to the inhibition

of accumulation of DdCAD-1 on the cell surface [20]. All of the evidence suggests that DdCAD-1 is transported to the cell surface by the CV and reveals a new function of the CV.

Although the CV primarily acts as an osmoregulatory organelle, it is also involved in Ca^{2+} regulation. Cyclic AMP-induced Ca^{2+}-influx in *Dictyostelium* is controlled by two major compartments, the IP_3-sensitive ER and a non-IP_3-sensitive intracellular compartment, the CV systems [21-24]. It has been shown that in *lvsA*$^-$ cells in which the CV structure is aberrant, the calcium influx is greatly reduced upon cAMP stimulation [23].

The CV system is enriched in membrane-associated V-ATPase and calmodulin and both are used as markers for the CV complex [14]. V-ATPase localizes to both the CV and the endosomal membranes but is much more enriched in the CV system (Figure 2) [12]. V-ATPase is a conserved enzyme in all eukaryotic cells that transforms the energy generated from ATP hydrolysis to active transport H^+. In turn, the transmembrane electrochemical potential of H^+ is used to transport other ions or macromolecules [25]. Generally, the major function of V-ATPase is to regulate the cytosolic pH and the uptake of cations such as Na^+, Ca^{2+}, and Cd^{2+} via H^+-driven antiport [26]. The function of V-ATPase on the CV membrane is unclear. It has been suggested that *Dictyostelium* V-ATPase functions to establish a proton gradient to transport other ions into CVs, resulting in an inward flux of water [16].

Several other molecules are associated with and regulate the CV system in *Dictyostelium*, including Rab11A, Rab14, LvsA, and Drainin [27-31]. Rab11A localizes to both vacuolar and tubular structures of the CV complex in *Dictyostelium*. Cells expressing dominant-negative Rab11A exhibit abnormal enlarged CV bladders in hypotonic buffer and are sensitive to low-osmolarity stress [27]. Rab14 localizes to the endo-lysosomal pathway and the CV membrane system. Cells expressing dominant negative Rab14 are defective in endocytosis, endosomal membrane flow, homotypic lysosome fusion, and hypo-osmotic regulation [11, 29, 32]. LvsA is a BEACH family protein and regulates the biogenesis of the CV. The *lvsA*$^{-}$ cells lack an intact CV system and are sensitive to hypotonic stress [28, 30]. Drainin is a TBC domain-containing protein and localizes only to the bladders of the CV. *drainin*$^{-}$ cells exhibit enlarged CV bladders and are sensitive to low-osmotic stress [31].

Although several putative regulatory components have been associated with the *Dictyostelium* CV system, little is known about how the proteins regulate CV function. Two driving forces have been proposed to regulate CV discharge: unconventional myosin and membrane tension. Calmodulin localizes to CV membranes and is suggested to interact with unconventional myosin in *Dictyostelium* [33]. Injection of anti-myosin I antibodies in *Acanthamoeba* led to the abortion of the CV contraction [34]. Thus, it is suggested that Calmodulin and unconventional myosin regulate the CV contraction though a “muscle-like” way. However, none of the myosin mutants exhibit CV defects

and no F-actin or myosin has been observed on the CV by EM in *Dictyostelium* [17]. Another model proposes that the membrane tension driven by the spontaneous curvature of the membrane forms the contraction force. The study of *Paramecium multimicronucleatum* revealed that the periodic rounding and slackening of the CV coincides with the membrane tension increase and decrease both *in vitro* and *in vivo,* suggesting the spontaneous curvature of the lipid bilayer membrane is involved in the periodic development of CV membrane tension [35, 36]. In *Dictyostelium*, the tubular and vesicular structures are interconvertible. It would not be unexpected that the CV membrane becomes strained when it charges and becomes round, since the membrane has been converted from a tubular to a spherical shape. Therefore, the natural tendency to resume the tubularity may be the driving force of the CV contraction [17].

BEACH Family Proteins

BEACH proteins are evolutionally conserved family proteins found in all eukaryotes. The first BEACH protein identified, LYST (lysosomal trafficking regulator), is associated with Chediak-Higashi syndrome (CHS), which is characterized by oculocutaneous albinism, bleeding defects, severe immunodeficiency, and peripheral neuropathy in humans and other mammals [37, 38]. The beige mouse provides the most important animal model for CHS [39]. At the cellular level, cells from CHS patients exhibit giant granules including the platelet dense body, the melanosome, and the

lysosome [38]. Individual BEACH proteins have distinct physiological roles and are involved in lysosome trafficking, cytokinesis, CV regulation, and apoptosis [28, 30, 37, 40-44].

All BEACH proteins share a similar domain structure at their C-terminus: a PH-like domain, a BEACH (for beige and CHS) domain, and WD40 repeats. All of the BEACH proteins except the FAN subgroup have a long N-terminus, exhibit little similarity between BEACH proteins, and most proteins are over 400 kD [45]. The BEACH domain is crucial for the normal function of these proteins. All of the natural mutations associated with CHS are non-sense or frame-shift mutations leading to the premature termination of the protein and the loss of the BEACH domain [38, 46]. Furthermore, the severity of the syndrome does not correlate with the length of the remaining LYST proteins and indicates the integrity of the whole protein is required for proper function [46]. The BEACH domain does not share any sequence homology with other domains in the database and the molecular function of this domain is still unknown. Jogl and colleagues reported the crystal structure of a BEACH protein, Neurobeachin [47]. The structure analysis revealed a prominent groove at the interface between a PH-like domain and a BEACH domain which might serve as a binding site to recruit their binding partners [47]. The PH-like domain of Neurobeachin has a strong interaction with the BEACH domain and the two domains might function as a single unit. A recent paper [48] confirmed the conclusion that the intramolecular interaction between the PH and

BEACH domains is critical for their function [48]. The same paper demonstrated that the BEACH protein FAN is targeted to the plasma membrane by specific binding of the PH domain to phosphatidylinositol-4,5-bisphosphate [PtdIns(4,5)P]. Thus, the PH-like domain in FAN has two functions, membrane targeting and interdomain interaction. FAN interacts with F-actin in TNF-stimulated cells and mediates filopodia formation through Cdc42 signaling [48].

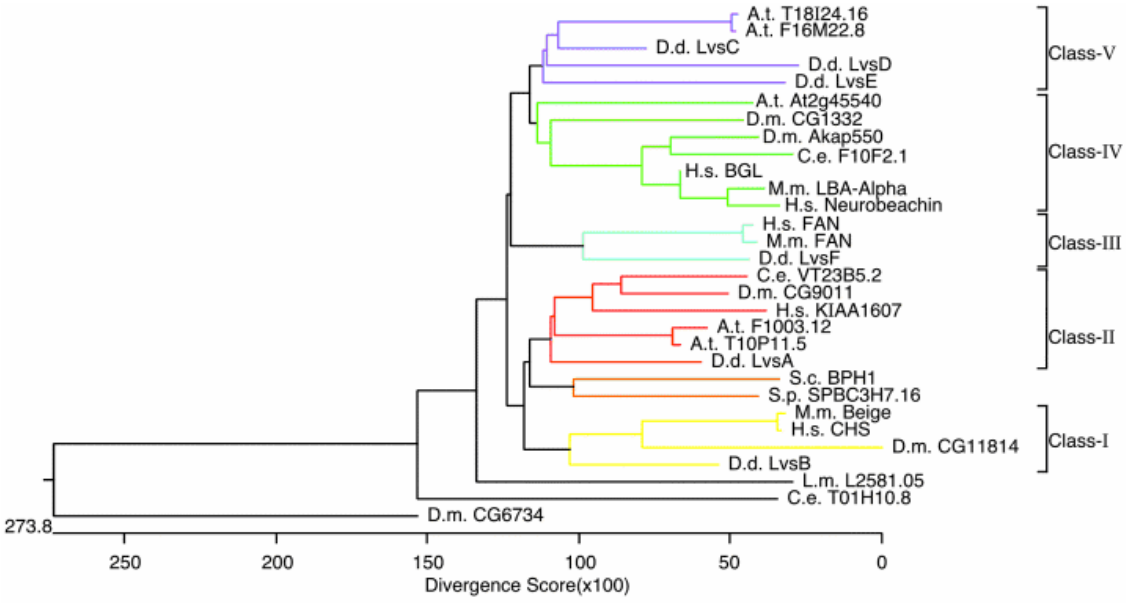

Figure 3:
Phylogenetic family tree of the BEACH proteins. The BEACH and WD40 domains of the indicated sequences were aligned by the clustalW algorithm and used to construct this phylogenetic tree. The image is adapted from paper [45] Figure 3.

In *Dictyostelium* there are seven BEACH proteins, LvsA-G (*Dictybase*). Loss of LvsA results in defects in cytokinesis, phagocytosis, and aberrant hypotonic response [28,

30, 41, 49]. LvsB is most closely related to LYST in *Dictyostelium* and plays a role in lysosomal trafficking [40, 49, 50]. No phenotypes have been linked to loss of LvsC-F [51]. By phylogenetic analysis of the conserved BEACH domain, BEACH proteins were clustered into five subgroups in all organisms, and *Dictyostelium* BEACH proteins fall into four of the five subgroups (Figure 3) [45]. Class I includes LYST and LvsB. LvsA belongs to Class II and FAN is a typical Class III protein which is the smallest BEACH protein without a long N-terminus. Class VI is represented by Neurobeachin and AKAP550 and both would interact with the regulatory subunit of PKA and might represent a novel class of A-kinase-adaptor proteins (AKAPs) [52, 53]. Class V is *Dictyostelium*- and *Arabidopsis*-specific, but is closely related to Class IV (Figure 3) [45].

Rab Proteins in *Dictyostelium*

Rab proteins belong to the Ras superfamily of small GTPase proteins, play central roles in regulating membrane trafficking, and are involved in all steps of vesicle transport, including vesicle formation, movement, tethering, and fusion with target membranes [54-56]. There are >60 Rabs in mammalian cells and 52 in *Dictyostelium* [57]. Phylogenetic analysis reveals that *Dictyostelium* has members in 13 of the 17 major Rab protein groups [57]. To date, 16 Rabs have been cloned in *Dictyostelium*, but only 5 of them have been linked to certain function [57]. Rab7A, Rab14, and Rab21 are involved

in phagocytosis [11, 29, 32, 58-62]. Rab7A and Rab14 also regulate lysosomal fusion [32, 63]. Rab11A and Rab14 are critical for CV function [27, 32]. Rab8A is involved in cell-cell adhesion, secretion, and actin protrusion formation [64].

Like all the other small GTPase, Rabs cycle between GDP-bound (inactive) and GTP-bound (active) states. The hydrolysis of Rab-GTP to Rab-GDP is stimulated by GTPase activating proteins (RabGAPs) and most RabGAPs contain a conserved catalytic TBC (Tre/Bub2/Cdc16) domain [65, 66]. Many studies have focused on the identification of Rab effectors, and far less is known about the GAPs that control Rabs because of the large number of Rabs and RabGAPs. A breakthrough was made recently by large scale screening, which allows the identification of some specific RabGAPs, such as Rab5-GAP, Rab27A-GAP (EPI64), Rab2A-GAP (OATL1), and Rab10-GAP (Evi5-like) [67-69]. In *Dictyostelium*, only one protein, DRG, has been shown to have RabGAP activity and stimulate the GTPase activity of both RacE and Rab14 [70]. Searching of the *Dictyostelium* database, I identified 29 TBC domain-containing ORFs.

Chemotaxis in *Dictyostelium*

Chemotaxis, or cell movement up a chemical concentration gradient, is critical in many physiological pathways, including innate immunity, angiogenesis, wound healing, embryogenesis, neuronal patterning, and morphogenesis. Many of the pathways that control the sensing of and responses to chemoattractant gradients are evolutionarily

conserved, allowing the use of model genetic systems to dissect these pathways. The social amoeba *Dictyostelium discoideum* is a powerful system in which to study chemotaxis due to the organism's distinct life cycle and the availability of genetic and cell biological tools to identify and dissect new regulatory pathways.

Starved *Dictyostelium* cells differentiate, polarize, and migrate directionally towards the secreted chemoattractant cAMP. Cyclic AMP is detected by the seven transmembrane receptor cAR1, which is uniformly distributed on the cell surface. Activation of the downstream heterotrimeric G protein leads to dissociation of the α and $\beta\gamma$ subunits, which regulate a series of downstream effectors, including Ras, phosphoinositide 3-kinase (PI3K), PTEN, adenylyl cyclase (AC), guanylyl cyclase (GC), and PLA_2. The signaling events eventually lead to either F-actin polymerization to generate pseudopod protrusion at the leading edge or Myosin II assembly for rear retraction and suppression of the lateral pseudopod [71].

F-actin polymerization occurs via a process called nucleation. Three main classes of proteins, actin-related protein 2/3 (Arp2/3), Spire, and Formins promote the initiation of new filament assembly. Both Spire and Formins promote the nucleation of unbranched filaments. The Arp2/3 complex initiates the formation of a new actin filament that branches off of an existing filament, generating Y-branched actin networks [72]. Arp2/3 is activated by WASP/WAVE/SCAR which in turn are activated by GTP-bound Rac [73-75]. In the absence of RacB, RacC, or RacGEF1, the specific exchange factor for

RacB, the F-actin polymerization is greatly reduced and cells exhibit chemotaxis defects [73, 76]. Interestingly, F-actin polymerization is not the end-point of chemotactic signaling. A positive feedback loop, mediated through localized F-actin polymerization, recruits cytosolic PI3K to the leading edge to amplify the signal and leads to further F-actin polymerization [77].

In *Dictyostelium*, stimulation with the chemoattractant cAMP causes an influx of Ca^{2+} and elevation of cytosolic Ca^{2+} [78-80]. The introduction of Ca^{2+} chelating buffers into the *Dictyostelium* cells inhibits cell chemotaxis [81]. Several actin-binding proteins, such as α-actinin， severin, fimbrin and ABP34 are calcium-dependent [82-84]. Inactivation of the Ca^{2+} binding site in EF hand I of α-actinin completely abolishes F-actin cross-linking activity in *Dictyostelium* [82]. Severin, an actin depolymerization protein, does not interact with actin filaments in the absence of Ca^{2+} [83]. Fimbrin and ABP34, the two actin-bundling proteins, display calcium-regulated bundling activity [84]. All of the evidence suggests that calcium is an important component in regulating chemotaxis. In higher eukaryotic cells, activation of many cell surface receptors causes the production of inositol 1,4,5-trisphosphate [InsP(3)], resulting in Ca^{2+} release from intracellular stores (usually ERs), via the $InsP_3$ receptor. Depletion of stores often triggers a larger influx of Ca^{2+} through the plasma membrane [85]. However, loss of function of the InsP(3) receptor-like gene, *iplA*, does not result in any chemotaxis defect in *Dictyostelium* [86]. A recent paper [87] confirmed that either blocking Ca^{2+} uptake with

EGTA or IP_3-mediated intracellular Ca^{2+} release in cells lacking the InsP(3) receptor has no effect on chemotaxis at low or high cAMP concentrations, suggesting that Ca^{2+} alone is not a central player in chemotaxis. However, chemotaxis mediated by PLA2, the pathway parallel to PI3K signaling, appears to be controlled by intracellular Ca^{2+}. Thus, inhibition of both the Ca^{2+} response and the PI3K pathway would completely inhibit the chemotaxis ability of the cells [87].

The MAP kinase cascade is a universal signaling unit used by a wide variety of eukaryotic signaling pathways and is composed of MEK kinase (MAP kinase kinase kinase, MEKK), MEK (MAP kinase kinase), and MAP kinase (ERK). The activation of this pathway involves serial phosphorylation and activation of the three kinases that leads to the phosphorylation of various cytoplasmic and nuclear protein substrates. MAPK pathways participate in chemotaxis regulation in both *Dictyostelium* and mammalian cells [88-91]. In *Dictyostelium*, the function of ERK1 in controlling aggregation and chemotaxis is unclear, but it is suggested to be the direct downstream effector of MEK1 because both *mek1* null cells and *erk1* null cells have similar chemotaxis defects and no ERK1 activity is detected in *mek1* null cells. Both *mek1* and *erk1* null cells are less elongated, forming lateral pseudopodia which cause them to move more slowly than wild-type cells during chemotaxis. Due to this chemotaxis defect, they both produce small aggregates and, as a result, the fruiting bodies formed are much smaller than in wild-type cells [92, 93].

A yeast-two-hybrid screen was performed to identify the ERK1 interacting proteins. A TBC domain-containing protein was identified in this screen which I designated as RabGAP1. *rabgap1*$^{-}$ cells exhibit higher F-actin polymerization upon cAMP stimulation, are more elongated, and move faster than wild-type cells during chemotaxis, which is the opposite of observations in *erk1*$^{-}$ cells.

By analyzing the independent knockout strains of *rabgap1*, I determined that RabGAP1 is involved in CV discharging by regulating CV/plasma membrane fusion. RabGAP1 localizes to the CV membrane at the late charging stage and *rabgap1*$^{-}$ cells have enlarged CVs. RabGAP1 and another TBC-domain-containing protein, Drainin, sequentially localize to the CV membrane and regulate CV discharge.

Two BEACH family proteins, LvsA and LvsD, were identified as a suppressor and an enhancer, respectively, in an REMI screening of the *rabgap1*$^{-}$ cells large vacuole phenotype. Using different strains, I characterized that LvsA and LvsD have distinct functions in regulating the biogenesis of CV and chemotaxis in *Dictyostelium*. This work increases our understanding of how CVs form and discharge and demonstrates that CV proteins are involved in chemotaxis through regulating F-actin polymerization.

ACKNOWLEDGEMENTS

This chapter, in part, is material to be submitted for publication in 2007, by Fei Du, Kimberly Edwards, Zhouxin Shen, Binggang Sun, Steven Briggs, Arturo De Lozanne, and Richard A. Firtel. Co-author Richard A. Firtel guided and supervised the writing of the introductory material.

Chapter II

A RabGAP Protein and BEACH Family Proteins Regulate Contractile Vacuole Formation and Activity and Chemotaxis in *Dictyostelium*

MATERIALS AND METHODS

Cell Culture

All *Dictyostelium* cells were grown in axenic HL5 medium. Knock-out cell lines were selected with either blasticidin or hygromycin but were maintained in HL5 medium once the cell lines were established. Overexpressing cells lines were maintained in HL5 with 20 μg/ml or 40 μg/ml G418 according to the expression level.

Gene Knock-out and Overexpression Constructs

I generated a *rabgap1* knockout construct by inserting the blasticidin or hygromycin resistance cassette into the *Bam*HI sites created at base 1196 of the *rabgap1* gene. *lvsD* was disrupted at base 6599 with either hygromycin or Cre-loxP blasticidin to generate multiple gene disruptions [94]. To knock out the *lvsA* gene, I used the re-circulated REMI construct to disrupt the gene at base 9393 and selected with blasticidin. The *rabgap1*, *dajumin,* and *lvsD* genes were amplified by PCR from Ax2 genomic DNA, cloned into the expression vector EXP-4(+) with either v5 or GFP or the RFP gene. All Rab genes were amplified by PCR from the *Dictyostelium* cDNA library and cloned into the RFP-EXP-4(+) vector. All mutations or deletions were generated using PCR. Successful mutagenesis was confirmed by sequencing. *drainin*$^{-}$ cells and LvsA^{OE} cells were from the De Lozanne lab.

Microscopy

All images were collected on a microscope (model DMIRE2; LEICA) with DIC and fluorescence imaging. All of the bright-field pictures were taken with a Hamamatsu C4742-95 camera with SimplePCI software under a 100X1.40 objective. All of the fluorescence pictures were taken under a 60X1.40 objective either with a Hamamatsu ORCA-ER C4742-80 camera for monochrome images or a Hamamatsu c9100 camera for two-color images.

GST-Pulldown Assay

The GST-pulldown assay was a modified protocol form Ras binding assay as described previously [77]. Briefly, GST or GST fused Rab proteins were produced in DE3 bacteria (Stratagene) and purified on glutathione-sepharose (Amersham Biosciences) according to the manufacturer's instructions. The amount of GST protein was measured by Coomassie-blue staining. The cell extract from *rabgap1*$^{-}$ cells expressing v5-RabGAP1 was incubated with 10 μg of GST or GST-Rab on glutathione-agarose beads at 4°C for 1 hour in the presence of 5 mg/ml BSA. The beads were washed three times. Proteins were separated on a 10% SDS-PAGE gel and immunoblotted with the anti-v5 antibody (Sigma). The input of GST-beads was measured by Commassie-blue staining.

Detection of the RabGAP1 Complex and Mass Spectrometry

Purification of the RabGAP1 complex and mass spectrometry were performed with modifications of protocols described previously [95]. Briefly, vegetative cells were washed with Na/K phosphate buffer and resuspended at a density of 4 x 10^7 cells/ml in Na/K phosphate buffer. Cells were lysed with 2X lysis buffer (1% NP-40, 300 mM NaCl, 40 mM MOPS, pH 7.0, 20% glycerol, 2 mM Na_3VO_4). Subsequently, cell lysates were incubated in 2.5 mg/ml DSP (dithio-bis-succinimidylpropionate, Calbiochem, La Jolla, CA). The cross-linking reactions were quenched with 200 mM Tris-HCl (pH 7.4) and protease inhibitors were added. After centrifugation, total cell extracts were immunoprecipitated with 25 µl resin of anti-V5 (V5–10) antibody agarose conjugate (Sigma). The immunoprecipitated products were eluted with buffer containing 4% SDS and 0.1 M glycine (pH 2.5) and the protein complex was incubated with 100 mM DTT and then precipitated with methanol/chloroform. The samples were washed with acetone, resuspended in Tris buffer, 8 M urea, pH 8.6, reduced with 100 mM TCEP, and alkylated with 55 mM iodoacetamide. Trypsin digest was done in the presence of 1 mM $CaCl_2$ for tryptic specificity. Peptide mixtures were loaded onto a triphasic LC/LC column with the following steps of 500 mM ammonium acetate bumps: 25, 35, 50, 80, and 100%. Tandem mass spectra were analyzed using DTA Select and the *Dictyostelium* sequence database

with the following filtering parameters for cross correlation scores 1.8 (+1), 2.8 (+2), and 3.5 (+3). Identities of specific bands were confirmed by sequence analysis.

REMI Screening

REMI suppressor/enhancer screening is a modification of the protocol used in [3]. Briefly, log-phase *rabgap1*$^{-}$ cells which have hygromycin resistance were electroporated with *Dpn*II and a REMI vector containing a blasticidin resistance cassette. The tranformants were selected in 10 μg/ml blasticidin and plated on SM agar with *Klebsiella aerogenes*. Colonies were picked into 96-well plates and visualized under phase-contrast microscopy for different sizes of vacuoles. Genomic DNA of candidate cells was purified, cut with a restriction enzyme, re-circulated, and transformed into SURE Electroporation-Competent cells (Stratagene) to allow the sequencing of the gene.

F-actin Polymerization Assay

F-actin polymerization and myosin II assembly were assayed as previously described [96]. Briefly, caffeine-treated, aggregation-competent cells were stimulated with 10 μM cAMP and, at the indicated times, aliquots of cells were lysed by addition of an equal volume of 100 mM MES (pH 6.8) buffer containing 1% Triton X-100, 5 mM EGTA, and 10 mM $MgCl_2$. The cytoskeletal pellet was collected by centrifugation, suspended in 2X sample buffer, and subjected to SDS−PAGE. Actin and myosin levels were determined by

densitometric analysis of scanned Coomassie-stained gels.

Chemotaxis Analysis

Chemotaxis analysis was performed as described previously [97]. Briefly, aggregation-competent cells were placed on a 30 mm Petri plate with a hole covered by a glass coverslip. A glass capillary needle filled with 150 μM cAMP solution was positioned and the response of the cells was recorded with a time-lapse video recorder and SimplePCI software. Computer analysis was done with DIAS software. At least five cells were analyzed and the chemotaxis assays were performed at least three times on separate days.

RESULTS

Identification of RabGAP1

MAPK pathways consist of a conserved set of three protein kinases that function sequentially to control a wide variety of cellular functions such as cell growth, transformation, apoptosis, and development [98-100]. Previous studies from the Firtel laboratory demonstrated that the MAPK pathway containing MEK1 and ERK1 plays a critical role in controlling pathways leading to chemotaxis and development in *Dictyostelium* [92, 93, 101, 102]. To identify the ERK1 interacting proteins, a yeast two-hybrid screen was performed. A protein (designated RabGAP1) containing a TBC domain, (the putative RabGAP domain) was identified. Disruption of the gene DDB0218275 resulted in cells exhibiting large vacuoles and having chemotaxis defects (see below).

The RabGAP1 contains a conserved F-box domain, a TBC domain, and a putative ERK binding motif, RERRMEESLKI (Figure 4A) [103]. Like other RabGAPs, the TBC domain of RabGAP1 has two conserved residues important for stimulating Rab GTPase activity, Arg^{515} and Gln^{551}, with a dual-finger mechanism [104-106]. Both residues have been mutated to alanines to disrupt the GAP activity to study the function of the TBC domain. Either of the mutations slows the rate of GTP hydrolysis and locks Rabs in an active conformation [69]. There is a nine hydrophobic amino acid stretch as LAAVFLLIL inside of the TBC domain (Figure 4B). This is similar to the domain found within

Figure 4:
Sequence analysis of *Dictyostelium* RabGAP1. (A) Schematic diagram of the domain structure of RabGAP1 and the relative position of the truncation constructs used in the study. (B) Amino acid sequence alignment of the TBC domain of RabGAP1 (DDB0218275, *D. discoideum*); Drainin (AAD00520, *D. discoideum*); TRE2 (P35125, *Homo sapiens*); RN-tre (Q92738, *H. sapiens*); Bub2 (P26448, *S. cerevisiae*); and Cdc16 (CAA50606, *S. pombe*). The two conserved catalytic arginines and glutamines for GAP activity are marked with asterisks. The red box shows the hydrophobic stretch. (C) Amino acid sequence alignment of the 70 amino acids upstream of the TBC domain of RabGAP1 (DDB0218275, *D. discoideum*); Drainin (AAD00520, *D. discoideum*); TRE2 (P35125, *Homo sapiens*); RN-tre (Q92738, *H. sapiens*); Epi64 (AAK35048, *Homo sapiens*); and Evi5-like (Q96CN4, *Homo sapiens*). Red boxes indicate negatively charged residues.

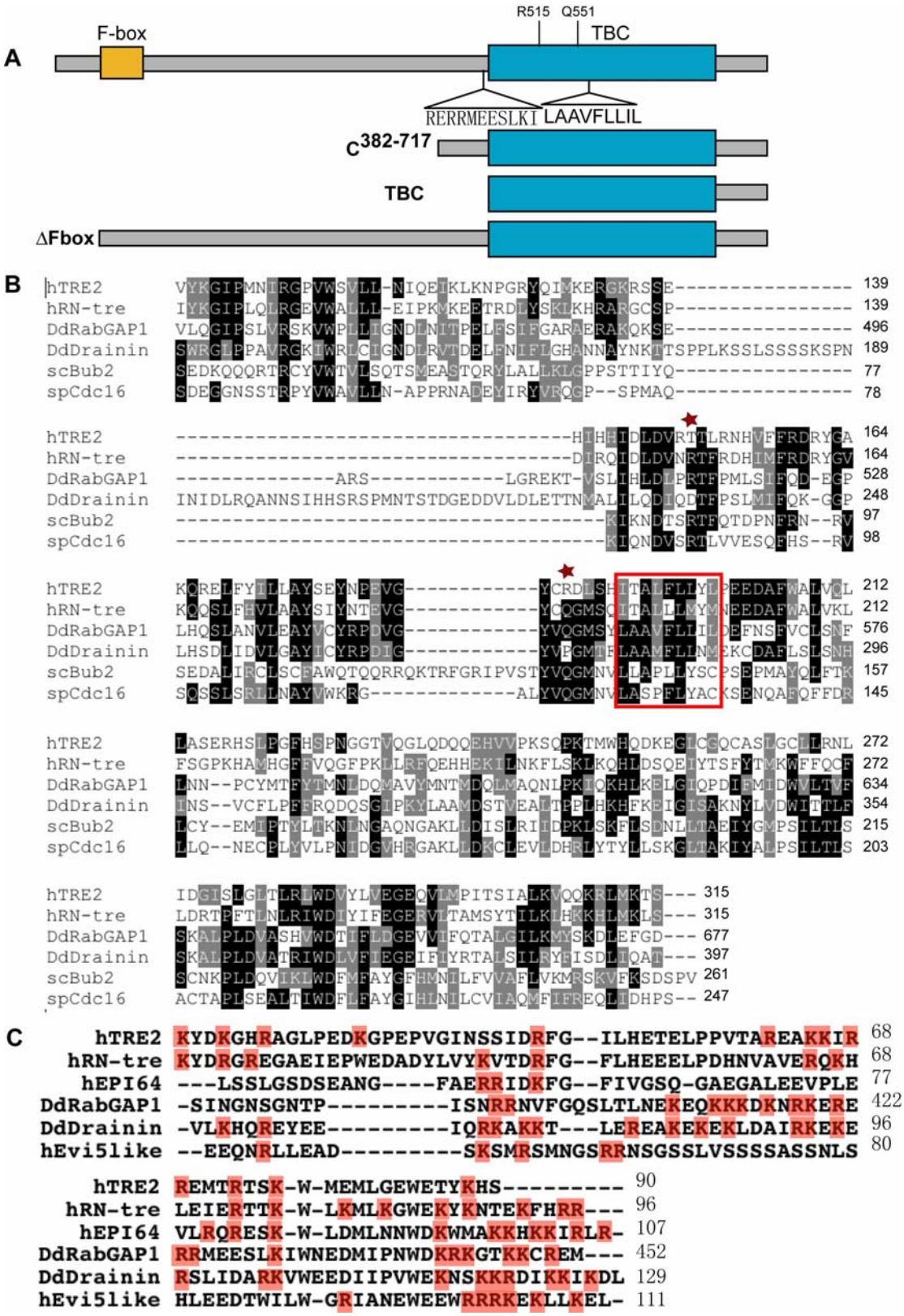
A
F-box
R515
Q551
TBC
RERRMEESLKT
LAAVFLLIL
C382-717
TBC
ΔFbox
B
hTRE2
hRN-tre
DdRabGAP1
DdDrainin
scBub2
spCdc16
C
hTRE2
hRN-tre
hEPI64
DdRabGAP1
DdDrainin
hEvi5like

Drainin, a previously identified CV protein, which, when deleted, causes enlarged CV bladder phenotype [31]. Interestingly, sequence comparison revealed that Drainin contains a TBC domain but lacks the conserved catalytic Arg and Gln, suggesting Drainin may not have GAP activity (Figure 4B). To determine the function of different parts of RabGAP1, I made several deletions and truncated proteins fused with GFP, including the deletion of the 9 hydrophobic amino acids (Δ9), a deletion of the F-box domain (ΔF-box), the TBC domain alone, and the fragment $C^{382\text{-}717}$ which contains the TBC domain and its upstream 70 amino acids (Figure 4A).

Although RabGAP1 was identified by its interaction with ERK1 in a yeast two-hybrid screen, I could not detect any interaction between RabGAP1 and ERK1 in co-immunoprecipitation experiments when tagged versions of both proteins were co-expressed in unstimulated or chemoattractant-stimulated cells. Expression of RabGAP1 with two sets of mutations in the ERK binding motif (R421A, R423A, R424A, and L429, I431A) (Figure 4A) did not cause any observed phenotype in wild-type cells and complemented the morphological phenotype of *rabgap1*$^{-}$ cells (data not shown). This finding suggests that the RabGAP1- ERK1 interaction might be an artifact of the yeast two-hybrid system.

Loss of RabGAP1 Causes the Formation of Large Vacuoles

To determine the function of RabGAP1, I generated *rabgap1* knockout strains by

Figure 5:
Cell morphology changed by disrupting the *rabgap1* gene. (A) The cell morphology of wild-type Ax2 and *rabgap1*$^{-}$ cells. Large vacuoles are indicated by arrows. (B) The cell morphology of *rabgap1*$^{-}$ cells expressing wild-type RabGAP1 or RabGAP1 with a ΔF-box deletion, RabGAP^{R151A} or RabGAP^{Q551A}, and Ax2 cells expressing RabGAP^{R151A} or RabGAP^{Q551A}. Large vacuoles are indicated by arrows. Scale bars, 10 μm. (C) Quantitation of the percentage of cells with different vacuolar sizes. The percentage of cells with vacuole size >= 8 μm, >= 6 μm, >= 4 μm, >= 2.5 μm, or <=2.5 μm for Ax2, *rabgap1*$^{-}$, RabGAP1^{R515A}/*rabgap1*$^{-}$, RabGAP1^{Q551A}/*rabgap1*$^{-}$, RabGAP1^{R515A}/Ax2, RabGAP1^{Q551A}/Ax2, *drainin*$^{-}$, *drainin*$^{-}$*/rabgap1*$^{-}$, LvsA^{OE}/*rabgap1*$^{-,-}$ and *lvsD*$^{-}$*/rabgap1*$^{-}$ strains. Vacuole size was measured by the diameter for the round vacuoles or the average of the length for the oval ones. The vacuole sizes of at least 100 cells from each cell line were measured.

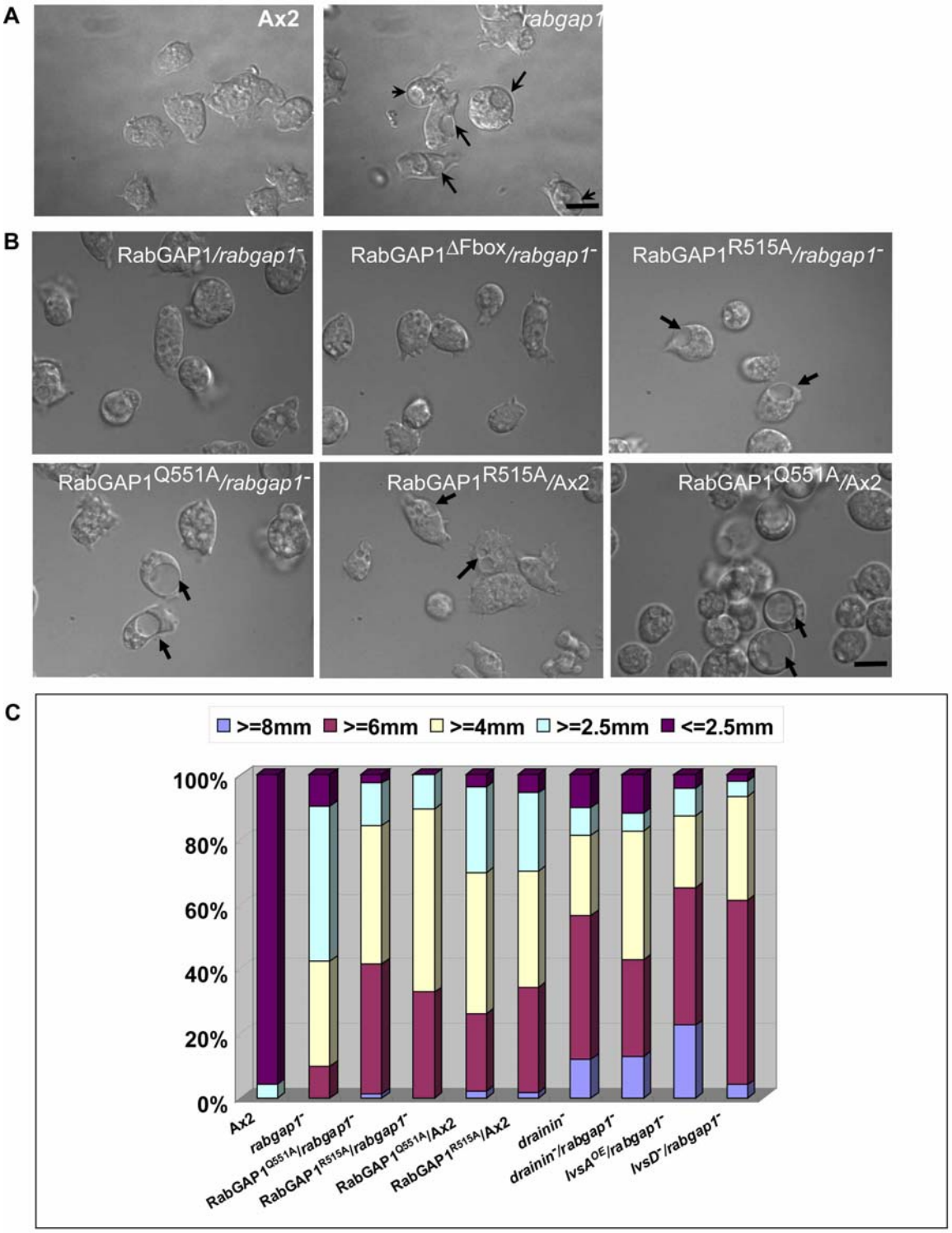
A
Ax2
rabgap1
B
RabGAP1/rabgap1-
RabGAP1ΔFbox/rabgap1-
RabGAP1R515A/rabgap1-
RabGAP1Q551A/rabgap1-
RabGAP1R515A/Ax2
RabGAP1Q551A/Ax2
C
>=8mm
>=6mm
>=4mm
>=2.5mm
<=2.5mm
100%
80%
60%
40%
20%
0%
Ax2
rabgap1-
RabGAP1Q551A/rabgap1-
RabGAP1R515A/rabgap1-
RabGAP1Q551A/Ax2
RabGAP1R515A/Ax2
drainin-
drainin-/rabgap1-
lvsAOE/rabgap1-
lvsD-/rabgap1-

homologous recombination. Independent knockout strains were identified by Southern blot and verified by Northern blot (data not shown). The *rabgap1*$^{-}$ clones exhibited large vacuole morphology (up to 7 μm) and was easily observed under phase-contrast or DIC microscopy (Figures 2A, 2C). Most wild-type (strain Ax2) cells contained no observable vacuole, even when observed under DIC microscopy. I detected some small vacuoles in ~12% of Ax2 cells, but only under DIC microscopy (Figure 5C).

Overexpressing full-length RabGAP1 in *rabgap1*$^{-}$ cells complemented the large vacuole phenotype (Figure 5B), as did a RabGAP1 lacking the F-box domain (RabGAP1$^{\Delta Fbox}$). However, RabGAP1 carrying point mutations in either of the conserved residues required for GAP activity (RabGAP1^{R515A}; RabGAP1^{Q551A}) did not complement the null mutations and produced even larger vacuoles when expressed in *rabgap1*$^{-}$ cells (up to 11 μm; Figures 2B, 2C). Expression of either RabGAP1^{R515A} or RabGAP1^{Q551A} in Ax2 wild-type cells also caused large vacuoles (Figures 2B, 2C), suggesting the protein exhibited a dominant negative effect. I expected that the enhanced phenotype resulted from dominant negative effects by further blocking the Rab intrinsic GTPase activity and/or competing for and binding to common substrates of another RabGAP. Alternatively, RabGAP1^{R515A} or RabGAP1^{Q551A} might bind to and compete with other essential components of the pathway. These findings indicate that RabGAP activity is required in the pathway regulating CVs and that the F-box domain is not essential for this process.

RabGAP1 Localizes to the Membrane of CVs

To examine the subcellular localization of RabGAP1, I cloned the full-length gene and created a GFP fusion which I expressed in *rabgap1*$^{-}$ and wild-type cells. GFP-RabGAP1 complemented the *rabgap1*$^{-}$ cell phenotypes. In both strains, RabGAP1 was found in the cytosol and on vacuole membranes (Figure 6A; data not shown). GFP-RabGAP1$^{\Delta Fbox}$ also localized to vacuole membranes, but the size of vacuoles was greatly reduced compared to the vacuole size in wild-type or *rabgap1*$^{-}$ cells expressing wild-type GFP-RabGAP1 (Figure 6A; data not shown). GFP-RabGAP1^{R515A} and GFP-RabGAP1^{Q551A} also localized to the vacuole membrane but vacuoles were enlarged (Figure 6A), consistent with the vacuole size observed under phase-contrast and DIC imaging (Figure 5B).

To determine the domains required for RabGAP1 localization to vacuoles, I created a series of deletion mutants (Figure 4A). GFP-TBC contained only the Rab GAP domain localized to cytoplasm and nucleus and did not complement the *rabgap1*$^{-}$ cell phenotypes (Figures 3B, 3C). However, a construct containing the TBC domain and the upstream 70 residues ($C^{382-717}$, Figure 4A), complemented the *rabgap1*$^{-}$ cell vacuole phenotypes and localized to the vacuole membrane and the plasma membrane, suggesting that the 70 residue region upstream of TBC domain was required for membrane localization (Figures 3B, 3C). The region of RabGAP1 between residues 382-452

upstream of the TBC domain is Arg and Lys rich. Drainin has a similar Arg/Lys-enriched region upstream of its TBC domain, as do several human RabGAPs, suggesting this is a conserved localization motif (Figure 4C).

I identified a conserved 9 residue hydrophobic stretch inside the TBC domain, LAAVFLLIL, similar to the one previously found in Drainin and shown to be required for vacuole localization (Figures 1A, 1B) [31]. RabGAP1 lacking these 9 residues (RabGAP1$^{\Delta 9}$) was cytosolic and did not rescue the *rabgap1*$^{-}$ cell vacuole phenotype (Figures 3B, 3C). Furthermore, expressing RabGAP1$^{\Delta 9}$ in wild-type cells resulted in larger vacuoles, although not as large as those observed in cells expressing RabGAP1^{R515A} or RabGAP1^{Q551A} (Figure 6C). Further sequence comparison indicates that the TBC domains of RabGAPs from yeast and mammals also have at least 5 hydrophobic residues in this region, I/L/VXXXF/I/LLL/M/YXL/M/C (Figure 4B). I suggest that this hydrophobic domain, along with the Arg/Lys-enriched domain, mediates vacuole targeting. These results suggest that RabGAP1 must localize to the vacuoles to mediate its functions.

To identify the property of the vacuoles to which RabGAP1 localizes, I labeled the cells expressing GFP-RabGAP1 with markers for different types of organelles. Cells expressing GFP-RabGAP1 were treated with either TRITC-Dextran for 2 hours or Lysotracker, or were co-expressed with RFP-Dajumin to visualize endosomes, lysosomes, and the CV system, respectively [19, 107, 108]. RabGAP1 only co-localized with

Figure 6:
RabGAP1 localizes to the membrane of CVs. (A) RabGAP1 localization in *rabgap1*$^{-}$ cells expressing GFP-RabGAP1, GFP-RabGAP1$^{\Delta Fbox}$, or GFP-RabGAP^{Q551A}. (B) Localization of truncated RabGAP1 in *rabgap1*$^{-}$ cells or Ax2 cells. (C) Cell morphology of *rabgap1*$^{-}$ cells or Ax2 cells expressing truncated RabGAP1. (D) Localization of GFP-RabGAP1 with markers for endosomes, lysosomes, or CVs. *rabgap1*$^{-}$ cells expressing GFP-RabGAP1 treated with either TRITC-Dextran for 2 hours to label endosomes, or with LysoTracker red DND-99 to mark lysosomes, or co-expressed with RFP-Dajumin for CV localization. (E) Localization of RFP-Dajumin (left panel) or GFP-RabGAP1 (right panel) in Ax2 cells under hypotonic stress. Pictures were taken simultaneously for both colors. Solid arrows indicate a discharge event and open arrows indicate a full charge and discharge cycle. Scale bars, 5 μm

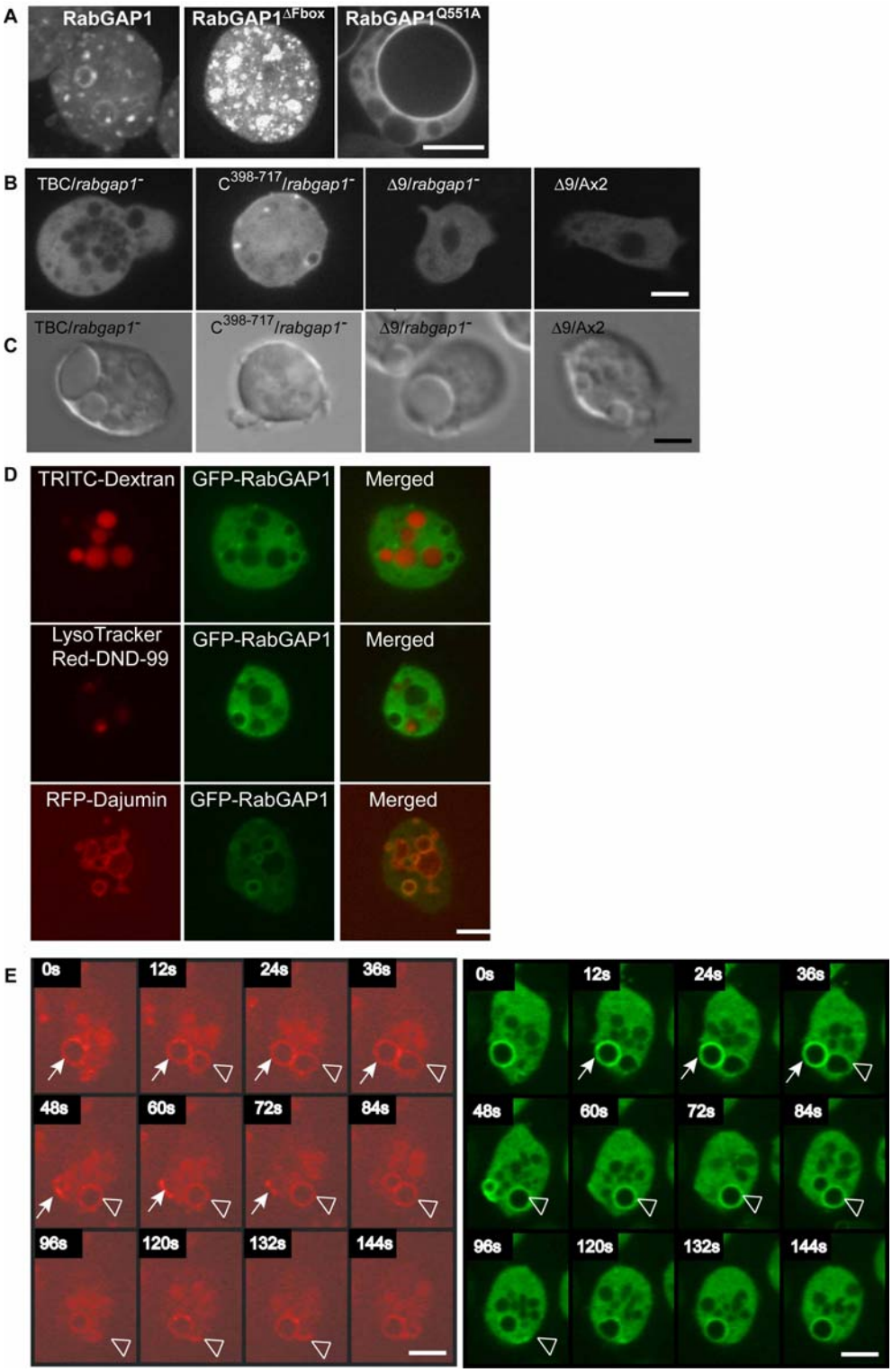
A
RabGAP1
RabGAP1ΔFbox
RabGAP1Q551A
B
TBC/rabgap1-
C398-717/rabgap1-
Δ9/rabgap1-
Δ9/Ax2
C
TBC/rabgap1-
C398-717/rabgap1-
Δ9/rabgap1-
Δ9/Ax2
D
TRITC-Dextran
GFP-RabGAP1
Merged
LysoTracker Red-DND-99
GFP-RabGAP1
Merged
RFP-Dajumin
GFP-RabGAP1
Merged
E
0s
12s
24s
36s
48s
60s
72s
84s
96s
120s
132s
144s

RFP-Dajumin, suggesting RabGAP1 was found in the CV system (Figure 6D). The CV system is the osmoregulatory organelle, consisting of bladder structures and a tubular network that collects and then eliminates excess water from *Dictyostelium* cells under hypotonic stress [16, 19]. RabGAP1 only localized to the bladder structures (Figures 3A, 3D). Interestingly, RabGAP1 did not mark all the vacuolar structures of the CV (Figure 6D). To understand the differences between the vacuoles with or without RabGAP1, I placed the cells co-expressing GFP-RabGAP1 and the CV marker RFP-Dajumin into water to activate the CV system. As expected, RFP-Dajumin marked evenly of all the vacuoles, and I could clearly observe the charging and discharging of the CVs (Figure 6E). However, RabGAP1 only localized to the membrane of CVs at late charging stage; the CV then stopped growing and I observed additional RabGAP1 localization to the CVs, prior to the fusion of the CV with the plasma membrane (Figure 6E). RabGAP1 dissociated from the plasma membrane immediately after the fusion, whereas Dajumin remained on the collapsed vacuole for an extended time (Figure 6E, 60s, 72s, 120s, and 132s time points). The time between RabGAP1 localization and the complete discharging of the vacuole was 57±18 seconds (n=30 cells), while the full cycle from the start of CV growth to discharging was 100±22 seconds (n=30 cells). This finding suggests that RabGAP1 might serve as a switch to move the vacuoles from the charging to the discharging stage.

Structure and Activity of the CV is Abnormal in *rabgap1*$^{-}$ Cells

Since RabGAP1 localized to CV bladders, I expected that the large vacuoles seen in *rabgap1*$^{-}$ cells were enlarged CV bladders. Using the CV marker RFP-Dajumin, I determined this was the case. In wild-type cells, Dajumin labeled both bladder and tubular structures of the CV system (Figures 3E, 4A). In *rabgap1*$^{-}$ cells, RFP-Dajumin clearly labeled the big vacuole structures corresponding to the ones observed under phase-contrast microscopy and the tubular structures were greatly reduced, proving that the tubular and vacuolar structures were interconvertable (Figure 7A). When I placed *rabgap1*$^{-}$ cells in low-salt buffer, the tubular structures were still fewer but the large vacuoles were no longer present; instead, I observed many smaller bladder structures (Figure 7A). In wild-type cells, the CV structures were still similar in both hypotonic and iso-tonic buffers (Figure 7A), suggesting that the CV activity changed in *rabgap1*$^{-}$ cells under hypotonic stress.

To compare the CV cycle, I placed wild-type cells or *rabgap1*$^{-}$ cells or the cells expressing the CV marker RFP-Dajumin in water. As previously described [16, 17, 19], when wild-type cells were placed in hypotonic conditions, the activity of the CV network increased and the charging and dynamic discharging of the vesicles by fusing to the plasma membrane were evident (Figures 3E, 4B, and 4D). After vacuole discharging, RFP-Dajumin remained as a patch on the plasma membrane, suggesting this membrane domain was distinct from the majority of the plasma membrane and might contain CV

Figure 7:

CVs' structure and activity are abnormal in *rabgap1*$^{-}$ cells. (A) CV structures in wild-type Ax2 cells and *rabgap1*$^{-}$ cells. Each picture represents a reconstruction of the 3D structure of cells expressing RFP-Dajumin. (B) Time course of CV discharging in Ax2 cells. Arrows indicate the bladder undergoes discharging through CV/plasma membrane fusion. (C) Time course of CV discharging in *rabgap1*$^{-}$ cells. Arrows indicate the bladder undergoes discharging. (D) Ax2 cells expressing RFP-Dajumin were placed in water and the localization of Dajumin was recorded. Open arrows indicate a full charge and discharge cycle which starts at the same discharge spot indicated by solid arrows. (E) *rabgap1*$^{-}$ cells expressing RFP-Dajumin were placed in water and the localization of Dajumin was recorded. (F) Time course of CV discharging in *rabgap1*$^{-}$ cells. The time frame indicates the minutes after water is added.

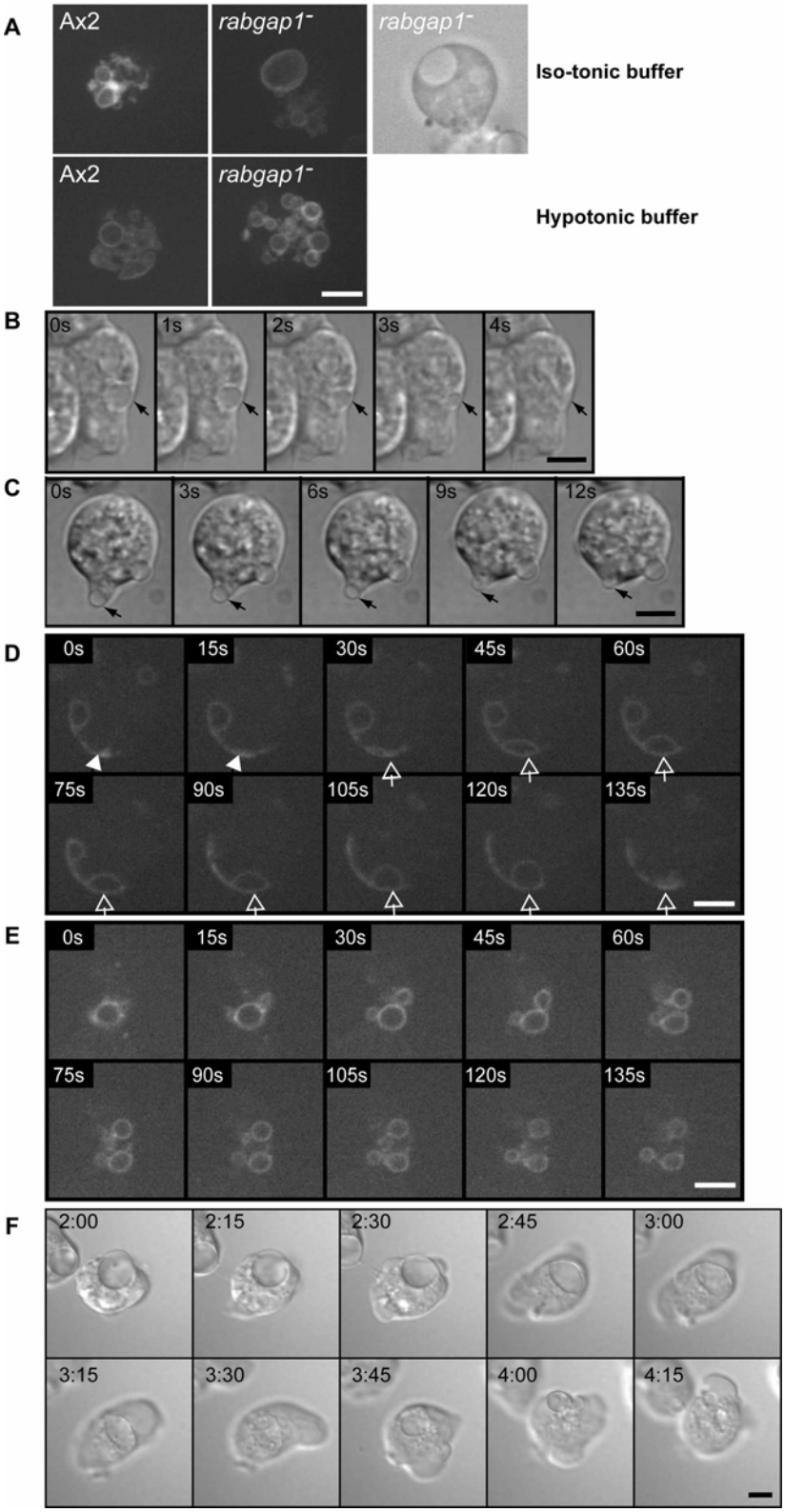
A
Ax2
rabgap1-
rabgap1-
Iso-tonic buffer
Ax2
rabgap1-
Hypotonic buffer
B
0s
1s
2s
3s
4s
C
0s
3s
6s
9s
12s
D
0s
15s
30s
45s
60s
75s
90s
105s
120s
135s
E
0s
15s
30s
45s
60s
75s
90s
105s
120s
135s
F
2:00
2:15
2:30
2:45
3:00
3:15
3:30
3:45
4:00
4:15

membrane components. Furthermore, as described previously [16], I found that new CV bladders preferentially formed at these sites (Figure 7D). When I placed *rabgap1*$^{-}$ cells in hypotonic medium, the large CVs disappeared within 5 minutes through the discharging of their contents and I observed no fusion of the CVs with the plasma membrane (Figure 7F). Numerous smaller vacuoles were present after the initial discharging of the large vacuoles (Figures 4C, 4E). These smaller vacuoles also discharged without fusing to the plasma membrane. Instead, the CVs rounded up and pushed out of the membrane (Figure 7C), a process not observed in wild-type cells (Figure 7B). At the end of this process, residual, small CV bladders remained, which withdrew inside of the cells (Figures 4C, 4E).

My observations suggest that RabGAP1 mediates CV discharging by regulating efficient vacuole/plasma membrane fusion. I suggest that the mechanism that underlies the formation of large vacuoles in *rabgap1*$^{-}$ cells in isotonic medium is that the vacuoles continue to grow (and possibly fuse), as they are unable to fuse with the plasma membrane. In developed *rabgap1*$^{-}$ cells, I observed active CV fusion (Figure 8A). I did not observe this in vegetative or developed wild-type cells, although this might be due to the fact that the vacuoles fused to the plasma membrane before they could fuse with each other.

rabgap1^{-} cells expressing RabGAP1^{Q551A} or RabGAP1^{R515A} placed under hypotonic stress exhibited even more extreme phenotypes. Some CVs appeared to

discharge for an extended time (>5 minutes in Figure 8B; data not shown) with GFP-RabGAP1^{Q551A} or GFP-RabGAP1^{R515A} remaining associated with the vacuole during this entire time. Eventually, smaller vesicles accumulated and discharged water a manner similar to that of vacuoles in *rabgap1*$^{-}$ cells (Figure 8C; data not shown).

Table 1:
Summary of the vacuole size and sensitivity to hypotonic stress of different cell lines. For vacuole size, - means no visible vacuoles in cells under phase-contrast microscopy, + means cells have large vacuoles, ++ and +++ mean cells have larger vacuoles than +. To measure the sensitivity to hypotonic stress, cells were placed in water for 2 hours and cell morphology was observed. - means cells still adhere to the substratum and are not sensitive to hypotonic stress, and + means cells round up, lyse, and are sensitive.

	Vacuole Size	Hypotonic stress
rabgap1^{-}	+	-
RabGAP1^{Q551A}/*rabgap1*$^{-}$	+++	-
RabGAP1^{R515A}/*rabgap1*$^{-}$	++	-
RabGAP1^{Q551A}/Ax2	++	-
RabGAP1^{R515A}/Ax2	++	-
RabGAP1$^{\Delta Fbox}$/*rabgap1*$^{-}$	-	-
lvsA^{-}	-	+
lvsA^{-}/*rabgap1*$^{-}$	-	+
lvsD^{-}	-	-
lvsD^{-}/*rabgap1*$^{-}$	+++	-
lvsA^{-}/*lvsD*$^{-}$	-	+
lvsA^{-}/*lvsD*$^{-}$/*rabgap1*$^{-}$	-	+
lvsA^{OE}	-	-
lvsA^{OE}/*rabgap1*$^{-}$	+++	-
lvsD^{OE}	-	-
lvsD^{OE}/*rabgap1*$^{-}$	-	-

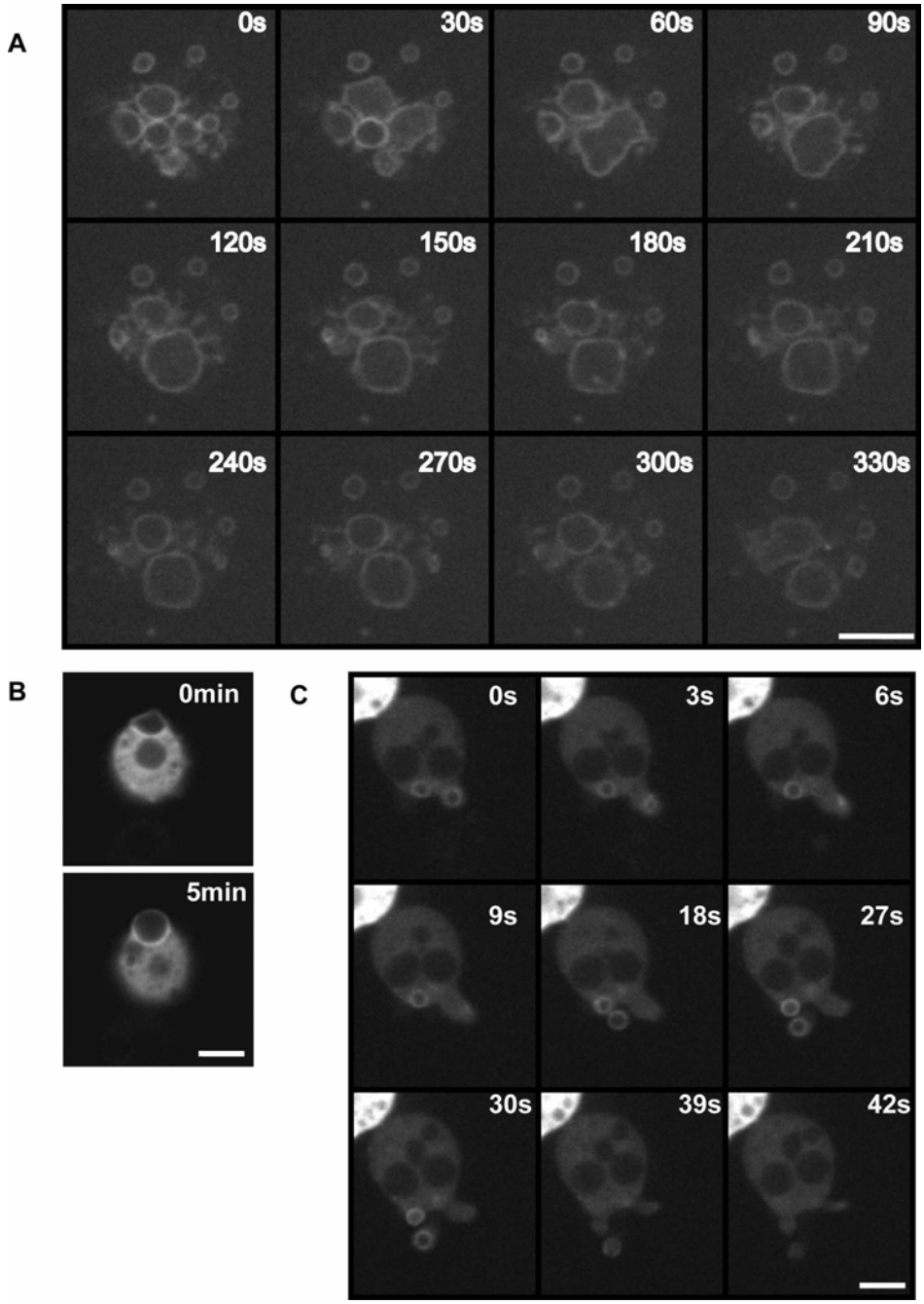

Figure 8:
CV membrane fusion and abnormal discharge. (A) Time course of localization of RFP-Dajumin in *rabgap1*$^{-}$ cells treated with 30 nM cAMP for 5 hours. (B) Localization of RabGAP1^{Q551A} in *rabgap1*$^{-}$ cells at 0 and 5 minutes in water. (C) Abnormal CV discharge in *rabgap1*$^{-}$ cells expressing GFP-RabGAP1^{Q551A} in water. Scale bars, 5 μm

Some strains exhibiting CV defects (e.g. *lvsA*$^{-}$ cells or cells expressing dominant-negative Rab14) are sensitive to hypo-osmotic stress, round up and swell before they eventually burst [11, 28]. Neither *rabgap1*$^{-}$ cells, nor RabGAP1 overexpressing cells, nor cells expressing RabGAP1^{R515A}, RabGAP1^{Q551A}, or RabGAP1$^{\Delta F\text{-box}}$ were sensitive to hypotonic stress (Table 1). This result was consistent with *rabgap1*$^{-}$ cells being able to discharge the contents of the CV.

Drainin and RabGAP1 Function Sequentially to Regulate CV Discharge

Although disrupting either *drainin* or *rabgap1* caused enlarged CV formation, the cell morphologies and the discharge of the CVs of the two mutant cells were not the same. The CVs were less enlarged in *rabgap1*$^{-}$ cells than in *drainin*$^{-}$ cells (Figure 5C). The vacuole sizes were more uniform in *rabgap1*$^{-}$ cells (few very large or small vacuoles), whereas in *drainin*$^{-}$ cells, the vacuole sizes were more variable and ranged from exhibiting no vacuole to having vacuoles as large as 12.5 μm (Figures 2C, 6A). *drainin*$^{-}$*/rabgap1*$^{-}$ cells exhibited a cell morphology similar to that of *drainin*$^{-}$ cells (Figure 5C). In *rabgap1*$^{-}$ cells, the active CV/plasma membrane fusion was absent but all cells could discharge. In *drainin*$^{-}$ cells, not all of the cells discharged, consistent with the previously observed partial osmotic sensitivity of the strain [31]. Of the *drainin*$^{-}$ cells that discharged, some formed membrane protrusions; in others, the vacuole formed a bleb as in *rabgap1*$^{-}$ cells, and in some cells, the vacuole fused to the plasma membrane as in

wild-type cells [31]. In *rabgap1*$^{-}$*/drainin*$^{-}$ cells, the discharge was similar to that observed in *drainin*$^{-}$ cells (data not shown).

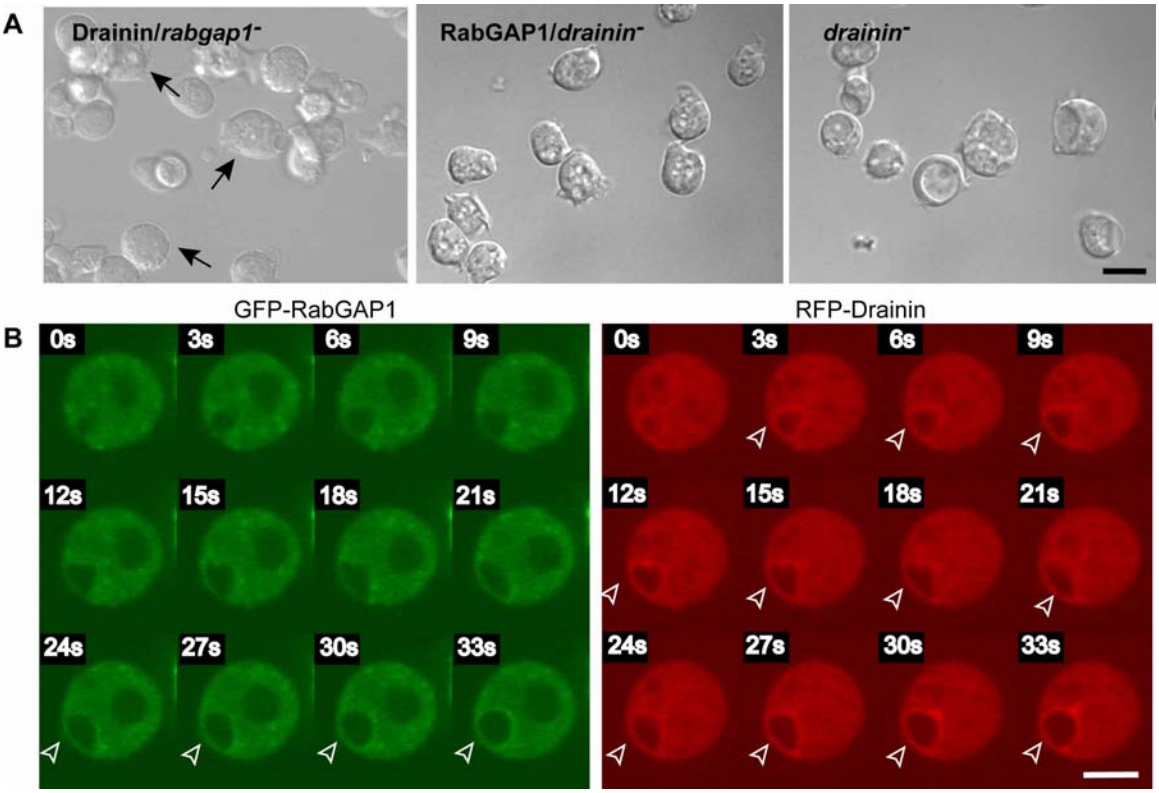

Figure 9:
Drainin and RabGAP1 function sequentially. (A) Cell morphology of Drainin/*rabgap1*$^{-}$, RabGAP1/*drainin*$^{-}$, and *drainin*$^{-}$ cells. In Drainin/*rabgap1*$^{-}$ cells, the cells expressing GFP-Drainin are indicated by arrows. All RabGAP1/*drainin*$^{-}$ cells express RabGAP1. Scale bar, 10 μm. (B) Localization of GFP-RabGAP1 and RFP-Drainin in *rabgap1*$^{-}$ cells under hypotonic stress. Pictures were taken simultaneously for both colors. Arrows indicate the time frames of RabGAP1 and Drainin association with CV bladders. Scale bar, 5 μm.

To investigate the relationship between these two proteins, I performed an epistasis experiment. Overexpressing RabGAP1 suppressed the large CV phenotype in

drainin^{-} cells (Figure 9A), although the discharging in those cells was still abnormal (data not shown). RabGAP1 still localized to CV bladders in *drainin*$^{-}$ cells, indicating Drainin was not required for RabGAP1 CV localization. Overexpressing Drainin in *rabgap1*$^{-}$ cells, however, did not suppress the *rabgap1*$^{-}$ large CV phenotype and the discharging was similar to that of *rabgap1*$^{-}$ cells (Figure 9A; data not shown). Drainin still localized to the CV bladders in *rabgap1*$^{-}$ cells (data not shown). The complementation data suggest that RabGAP1 might lie downstream of Drainin.

To examine the temporal localization of RabGAP1 and Drainin, I placed cells co-expressing GFP-RabGAP1 and RFP-Drainin in water and examined the protein localization. Drainin localized to the CV bladder prior to RabGAP1 (Figure 9B). This result and the complementation data strongly suggest that Drainin lies upstream from RabGAP1 to control vacuole size.

Rabs Regulated by RabGAP1

Since RabGAP activity is required in the pathway for normal vacuolar size in RabGAP1 pathway, I expect that some of the phenotypes of *rabgap1*$^{-}$ cells result from a specific Rab GTPases remaining in the GTP-bound form for an extended time. There are 52 Rabs in *Dictyostelium* [57]. Rab11A localizes to both tubules and bladders of the CV, while Rab14 only localizes to tubular structures of the CV [11, 27, 29, 32]. As expected, I found that Rab11A co-localizes with RabGAP1 and, like Dajumin, was found

constitutively on the CV. However, I observed that Rab14 lacked a distinct CV tubule or vesicle localization (Figure 10A). Expression of Rab11A in *rabgap1*$^{-}$ cells suppressed the large vacuole phenotype (Figure 10B), possibly by supplying a sufficient level of Rab11A-GDP to the CV system. This finding suggests that cycling of Rab11A is important for proper CV function. Unlike RabGAP1, Rab11A did not appear in the cytosolic pool and was only membranous, but the densities of Rab11A and RabGAP1 in different CVs were not the same (Figure 10A). Co-localization studies using *rabgap1*$^{-}$ cells co-expressing Rab11A and GFP-RabGAP1 demonstrated that RabGAP1 localized to the CV later than Rab11A (Figure 10C). The localization of constitutively activated Rab11A (Rab11A^{Q72L}) was similar to that of wild-type Rab11A and expressing Rab11A^{Q72L} did not yield any visible phenotypes in either wild-type or *rabgap1*$^{-}$ cells (data not shown).

I also studied 7 other Rabs, Rab5A Rab5B, Rab6A, Rab7A, Rab7B, Rab8A, and Rab21, all of which have been linked to vacuolar structures in *Dictyostelium* and/or other systems [57, 109]. Of these, only Rab8A co-localized with RabGAP1. Rab8A had exactly the same localization as RabGAP1 and exhibited the same relative intensity of staining on the CV bladder structures (Figure 10A). Like Rab11A, overexpression of Rab8A in *rabgap1*$^{-}$ cells suppressed the steady-state accumulation of large vacuoles (i.e. large vacuoles did not accumulate, Figure 10B), possibly by supplying a sufficient level of Rab11A or 8A-GDP to the CV system. However, neither Rab8A nor Rab11A suppressed

the abnormal discharge of CV in *rabgap1*$^{-}$ cells (data not shown), indicating the transition

Figure 10:
Rab8A and Rab11A are regulated by RabGAP1. (A) Localization of GFP-RabGAP1 with RFP-Rab11A, RFP-Rab14, and RFP-Rab8A. Scale bar, 5 μm. (B) The cell morphology of Rab8A/*rabgap1*$^{-}$, Rab11A/*rabgap*$^{-}$, Rab8A/*drainin*$^{-}$ and Rab11A/*drainin*$^{-}$ cells. Scale bar, 10 μm. (C) Localization of RFP-Rab11A and GFP-RabGAP1 in Ax2 cells under hypotonic stress. Arrows indicate the time frames of RabGAP1 and Rab11A association with CV bladders. Scale bar, 5 μm.

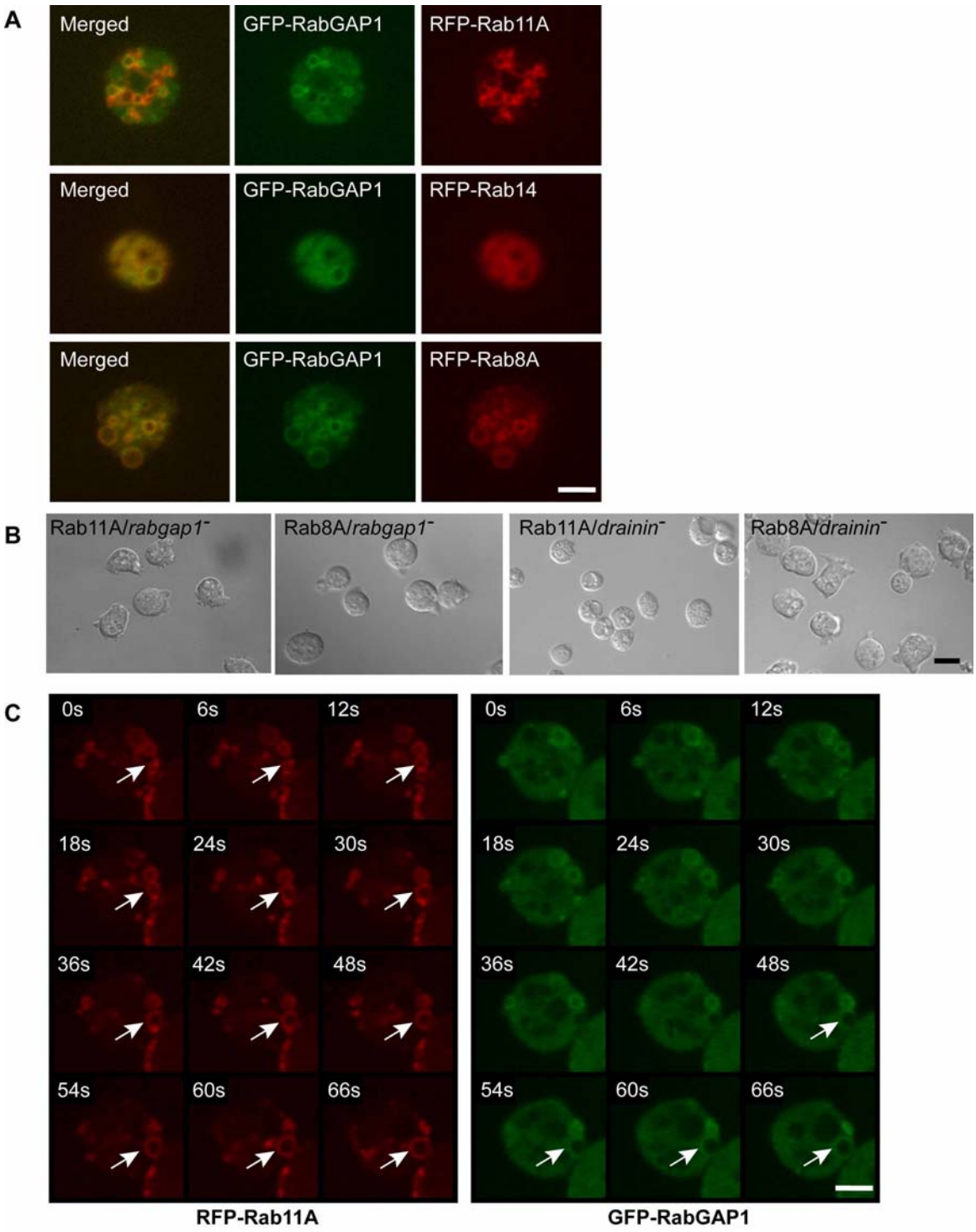
A
Merged
GFP-RabGAP1
RFP-Rab11A
Merged
GFP-RabGAP1
RFP-Rab14
Merged
GFP-RabGAP1
RFP-Rab8A
B
Rab11A/rabgap1-
Rab8A/rabgap1-
Rab11A/drainin-
Rab8A/drainin-
C
0s
6s
12s
18s
24s
30s
36s
42s
48s
54s
60s
66s
RFP-Rab11A
GFP-RabGAP1

from the GTP-bound to the GDP-bound form was important to fulfill Rab function. To address the relationship between RabGAP1 and Rab8A, I co-expressed these two proteins and examined their activity under hypotonic stress. Under my assay conditions, Rab8A and RabGAP1 co-localized and translocated to the CV membrane contemporaneously within the limits of our microscopy system. Both were recruited to the CV membrane at the end of charging stage and/or in the beginning of discharging stage (Figure 11A). Rab8A still localized to CV bladders in *rabgap1*$^{-}$ cells, as in wild-type cells (data not shown), indicating RabGAP1 was not required for Rab8A recruitment to the CV membrane. As I have not succeeded in generating a Rab8A knockout, I have been unable to test a dependency for RabGAP1's localization on Rab8A. When I overexpressed Rab8A^{ca}, or expressed it together with Rab11A^{ca} in wild-type cells, I did not observe enlarged CV bladders as seen in *rabgap1*$^{-}$ cells (data not shown). These results indicate that RabGAP1 might regulate other Rabs and/or RabGAP1 might have other functions independent of its GAP activity that were required for proper CV discharge, possibly acting as a Rab effector.

Interestingly, Rab8A, but not Rab11A, rescued the large CV phenotype in *drainin*$^{-}$ cells (Figure 10B). Furthermore, expressing Rab8A suppressed the abnormal discharge in *drainin*$^{-}$ cells (data not shown). Thus, Rab8A may be a direct regulator of vacuole/plasma membrane fusion during discharging.

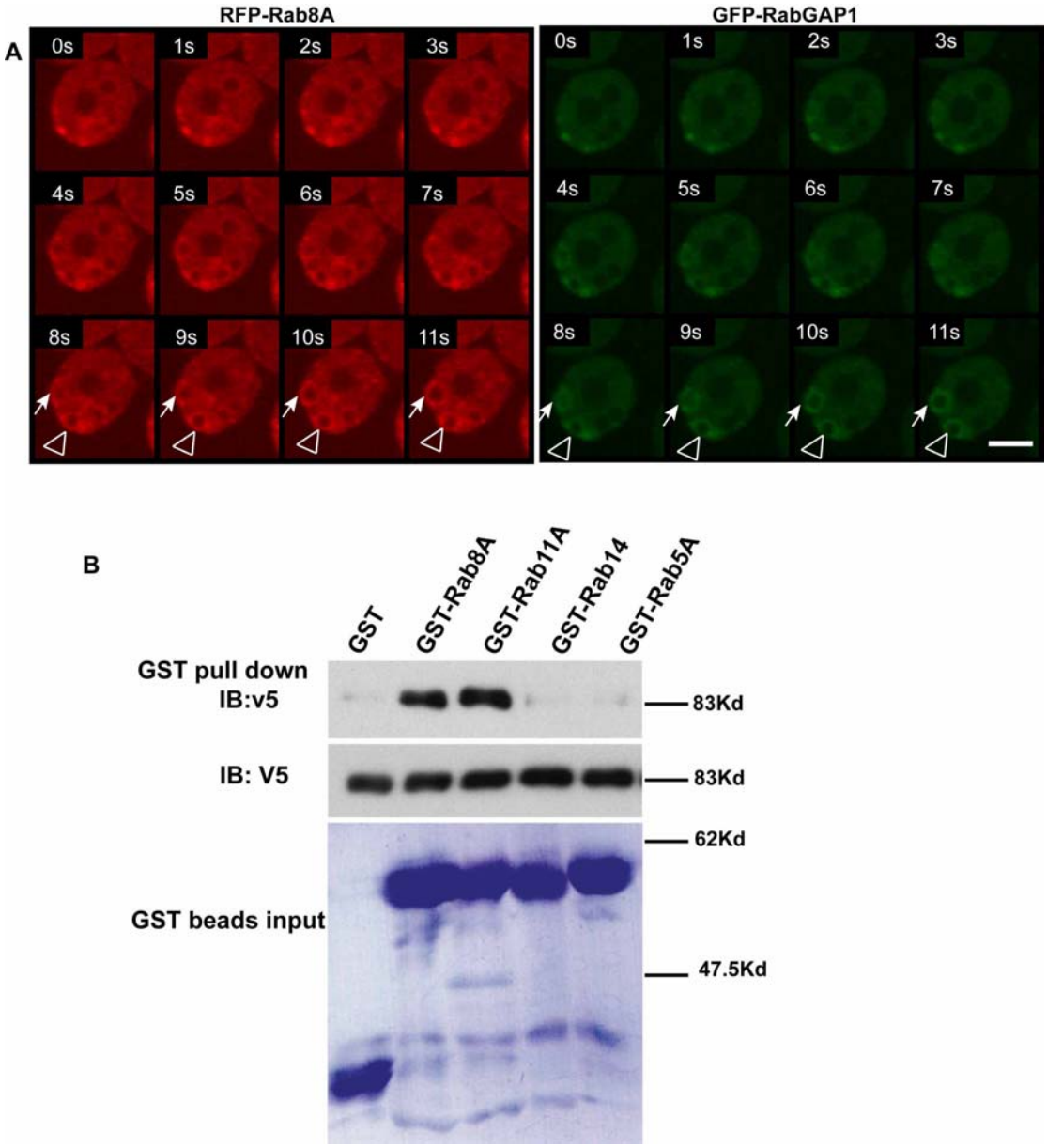

Figure 11:

Co-localization and interaction of Rab8A with RabGAP1. (A) Localization of RFP-Rab8A and GFP-RabGAP1 in Ax2 cells under hypotonic stress. Arrows indicate the time frames of Rab8A and RabGAP1 association with CV bladders. Scale bar, 5 μm. (B) GST pull-down assay of RabGAP1. Purified glutathione beads conjugated with GST, GST-Rab5A, GST-Rab8A, GST-Rab11A, or GST-14 were incubated with a cell lysate expressing v5-RabGAP1. The products were probed with an anti-v5 antibody. Input of v5-RabGAP1 and GST beads is indicated below the two bottom panels.

To test whether Rab8A, Rab11A, or Rab14 were the potential *bona fide* Rabs regulated by RabGAP1, I performed a GST pull-down assay using GST, GST-tagged Rab5A, Rab8A, Rab11A, and Rab14. Rab5A, serving as a negative control, localizes to endosomes and should not interact with RabGAP1. As shown in Figure 11B, Only Rab8A and Rab11A but not Rab14 or Rab5A or GST alone pulled down v5-tagged RabGAP1.

REMI Suppressor/Enhancer Screening of *rabgap1*$^-$ Cells

To identify other potential components in the pathway regulated by RabGAP1, I undertook an insertional mutagenesis (REMI using a Blasticidin resistance cassette) screen for second site suppressors and enhancers of the *rabgap1*$^-$ cell vacuolar phenotype by identifying clones exhibiting a change in vacuolar size with phase-contrast microscopy. Visual screening of ~7000 clones yielded 11 candidates with a changed vacuolar morphology; of these, only 5 retained Blasticidin resistance (Bs^R). One strain (#4-1) exhibited a suppression of the large vacuole phenotype, 2 strains (#2237-2, -3) had even larger vacuoles than *rabgap1*$^-$ cells, and 2 other strains (#15-1, -2) had smaller cells with smaller vacuoles (Figure 12A). After recircularizing and cloning the insertion site of the Bs^R cassette from the suppressor and enhancer clones, I found that *lvsA* (DDB0191124) had been disrupted in strain #4-1 and *lvsD* (DDB0185108) was disrupted in the 2 strains exhibiting larger vacuoles. I was unable to clone the insertion site of the other 2 strains.

I confirmed the knockout phenotypes by creating independent gene knockout

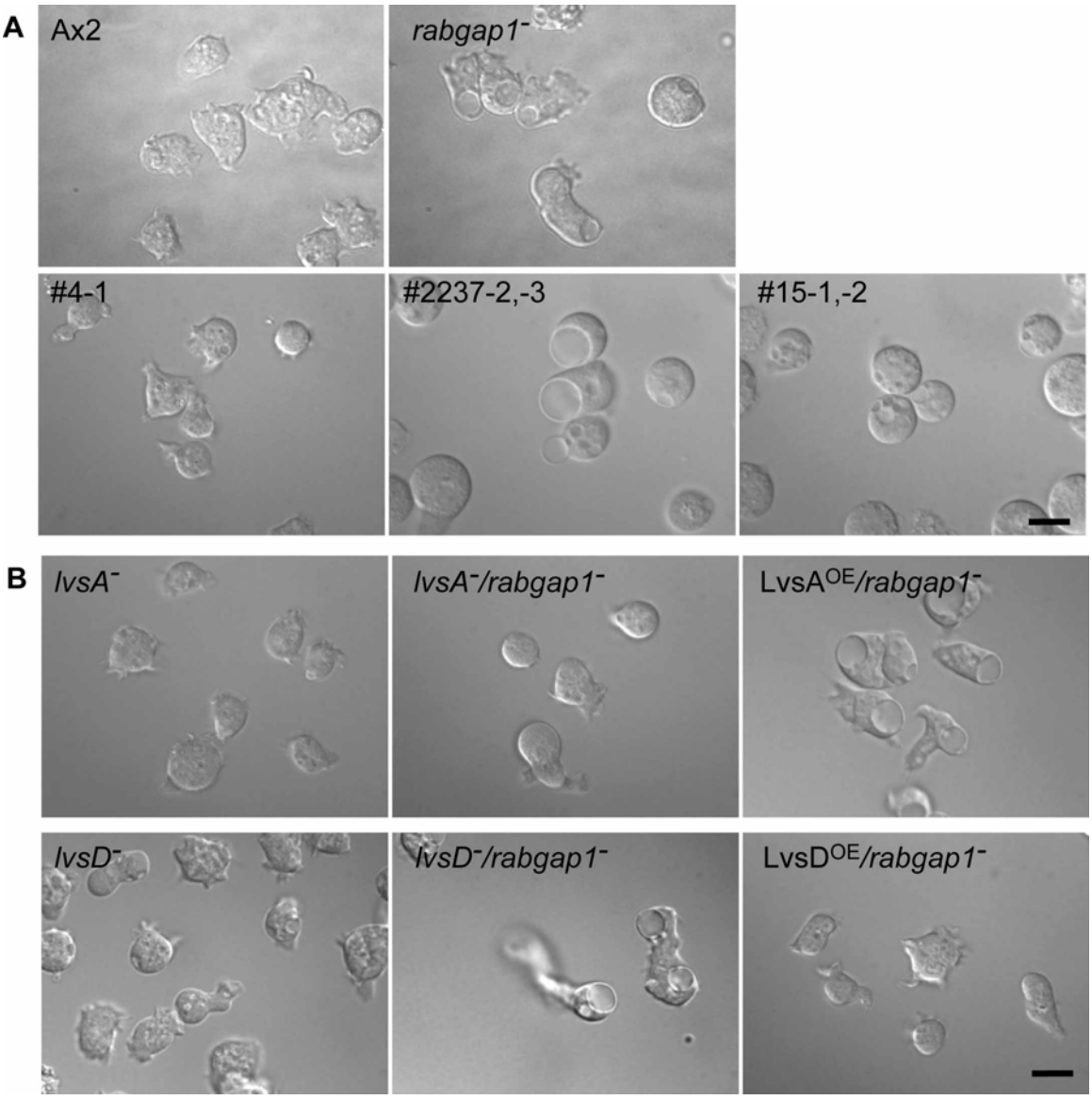

Figure 12:
lvsA and *lvsD* genes derived from REMI screening of *rabgap1*$^{-}$ cells。 (A) Cell morphology of different REMI clones, Ax2, and *rabgap1*$^{-}$ cells. (B) Cell morphology of *lvsA*$^{-}$, *lvsD*$^{-}$, *lvsA*$^{-}$*/rabgap1*$^{-}$, *lvsD*$^{-}$*/rabgap1*$^{-}$, LvsA^{OE}*/rabgap1*$^{-}$, and LvsD^{OE}*/rabgap1*$^{-}$. Scale bars, 10 μm.

constructs for *lvsA* and *lvsD* and disrupting the genes in *rabgap1*$^{-}$ cells. As depicted in Figure 12B, disruption of *lvsA* in *rabgap1*$^{-}$ cells suppressed the *rabgap1*$^{-}$ cells' large

vacuole phenotype, whereas the phenotype was enhanced when *lvsD* was disrupted (Figures 2C, 9B; Table 1).

LvsA and LvsD are BEACH family proteins [28, 30, 41, 45, 49, 51]. We confirmed that disruption of *lvsA* caused loss of visible CVs and tubules (Figure 13A), whereas loss of *lvsD* (in a wild-type background) did not produce a visible phenotype (Figure 12B) [51]. Cells in which the endogenous promoter of *lvsA* has been replaced by a more active actin promoter and GFP to create a GFP-LvsA-knock-in overexpressed GFP-LvsA (LvsA^{OE} cells) as determined by Western blot analyses using an anti-LvsA antibody [28]. These cells did not exhibit a vacuolar phenotype; however, disruption of *rabgap1* in this background (LvsA^{OE}*/rabgap1*$^{-}$) led to an enhanced, enlarged vacuole phenotype, similar to observations in cells lacking *rabgap1* and *lvsD* (*lvsD*$^{-}$*/rabgap1*$^{-}$) (Figures 9B, 2C; Table 1). Overexpressing LvsD in *rabgap1*$^{-}$ cells suppressed the *rabgap1*$^{-}$ cells' large vacuole phenotype (Figure 12B). These results indicate that LvsA and LvsD regulate the CV system but have very distinct, and possibly opposite, functions.

LvsA and LvsD Maintain the Integrity of the CV System

To visualize the CV and examine its activity, I expressed RFP-Dajumin in different Lvs/RabGAP1 strains. I confirmed that no bladder or tubular structures were observed in *lvsA*$^{-}$ cells; only small punctate structures were seen with Dajumin labeling (Figure 13A) [28, 30] suggesting that a functional CV system was absent. This was

consistent with the observations that *lvsA*$^{-}$ cells were sensitive to hypo-osmotic shock, (Table 1) [28]. *lvsA*$^{-}$*/rabgap1*$^{-}$ cells exhibited a similar phenotype (Figure 13A; Table 1). V-ATPase still localized to these punctate structures, suggesting that in the absence of LvsA, early or immature CV structures formed but could not mature or enlarge [28].

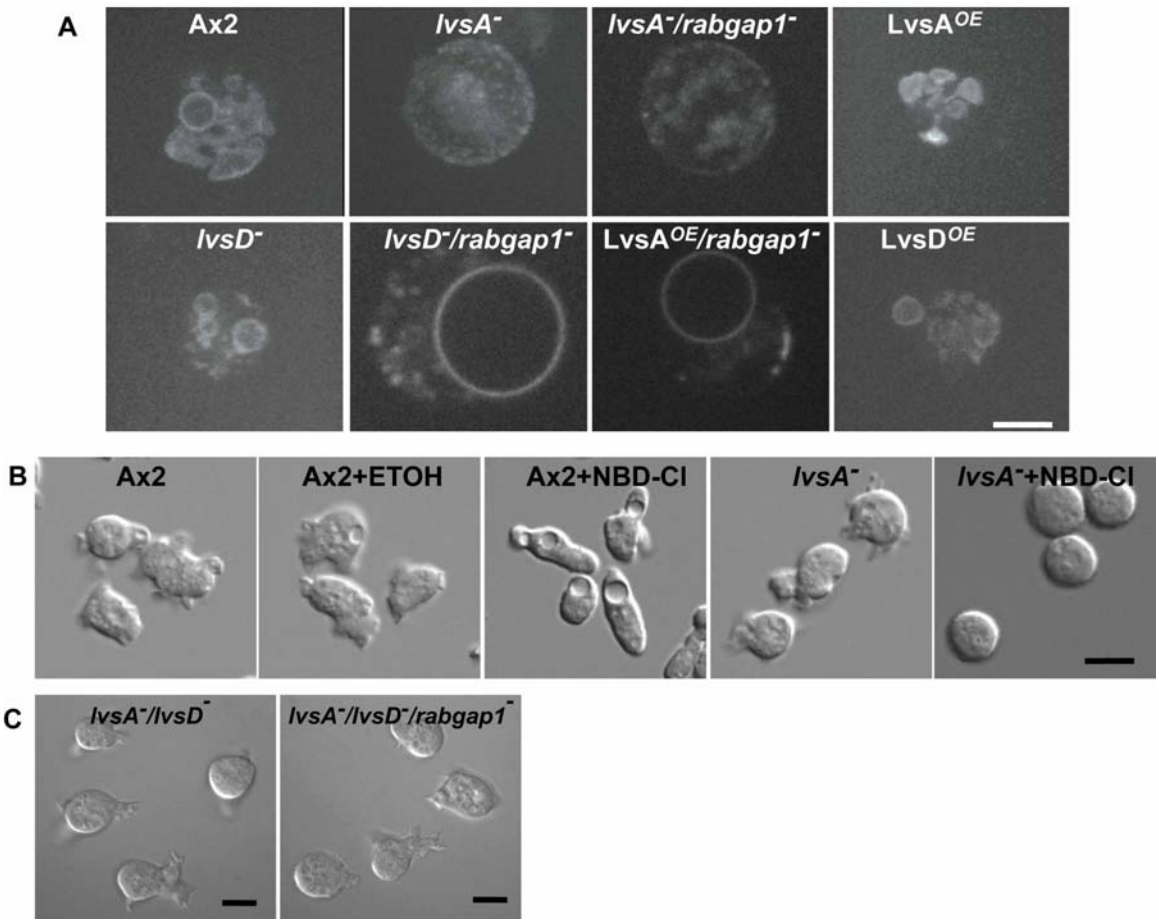

Figure 13:
LvsA and LvsD maintain the integrity of CVs. (A) Localization of RFP-Dajumin in different cell lines. Scale bar, 5 μm. (B) Cell morphology changes in cells treated with NBD-Cl. Ax2 and *lvsA*$^{-}$ cells were treated with EtOH or NBD-Cl. Scale bar, 10 μm. (C) Cell morphology of *lvsA*$^{-}$*/lvsD*$^{-}$, and *lvsA*$^{-}$*/lvsD*$^{-}$*/rabgap1*$^{-}$. Scale bar, 10 μm.

In LvsA^{OE} cells, there was an increase in the number of CV bladder structures compared to wild-type cells (Figure 13A). With the combination of the increase of the bladders by overexpressing LvsA and dysfunction of CV/plasma membrane fusion by disrupting *rabgap1* gene, the bladders were further enlarged in LvsA^{OE}/*rabgap1*$^{-}$ cells compared to the ones in *rabgap1*$^{-}$ cells (visualized by DIC imaging and GFP-Dajumin) (Figures 9B, 10A). In those cells, large vacuoles were present and the tubular structures were absent (Figure 13A), which further confirmed the theory that the tubular and vacuolar structure were interconvertible [15]. *lvsD*$^{-}$ cells appeared to have more bladder structures and a more reduced tubular network than wild-type cells, as observed by RFP-Dajumin fluorescence (Figure 13A). Thus, in the absence of functional RabGAP1, disrupting *lvsD* led to a further enlargement of vacuoles by shifting the equilibrium between bladder and tubular structures to bladders. In both *lvsD*$^{-}$ and LvsA^{OE} cells, CV charging and discharging activity appeared normal (data not shown). Furthermore, these strains were not hypo-osmotic-sensitive, indicating the CVs were functional (Table 1). In cells overexpressing LvsD, the CV structure was similar to that in wild-type cells (Figure 13A).

NBD-Cl is a specific inhibitor of V-ATPase and blocks CV activity. NBD-Cl-treated wild-type cells become swollen and have a round morphology in low-salt buffer and, eventually, lyse [20]. To examine the effect of NBD-Cl on the CV structure, I treated cells with NBD-Cl in the isotonic culture medium. Under these

conditions, the cells adhered less to the substratum and developed large vacuoles which were characterized as CVs by Dajumin labeling (Figure 13B; data not shown). This effect was not observed for control cells treated with 0.2% EtOH, the NBD-Cl solvent (Figure 13B). These observations suggest that V-ATPase is not required for the charge but is necessary for the discharge of the CV system. After the NBD-Cl treatment, *lvsA*$^{-}$ cells rounded up but did not exhibit any large vacuoles, consistent with LvsA being required for CV bladder formation (Figure 13B).

Since the fundamental function of LvsA is to maintain the integrity of the CV system, I would expect *lvsA*$^{-}$*/lvsD*$^{-}$ and *lvsA*$^{-}$*/lvsD*$^{-}$*/rabgap1*$^{-}$ cells to also lack visible bladders. Figure 13C shows this was the case: *lvsA*$^{-}$*/lvsD*$^{-}$ and *lvsA*$^{-}$*/lvsD*$^{-}$*/rabgap1*$^{-}$ cells lacked detectable vacuoles under phase-contrast or DIC microscopy (Figure 13C) and RFP-Dajumin labeling revealed the punctate structures seen in *lvsA*$^{-}$ cells (data not shown). Furthermore, these two strains exhibited all of the phenotypes of *lvsA*$^{-}$ cells, including sensitivity to hypotonic stress as well as phagocytosis and cytokinesis defects (data not shown) [28, 41].

Genetic Interactions between LvsA, LvsD, and RabGAP1

Time-lapse video microscopy revealed that the cycle of CV charging and discharging took ~100 seconds (Figures 3E, 4D and 11A) with the association of RabGAP1 and Rab8A with the CVs occurring at ~1 minute after vacuole charging

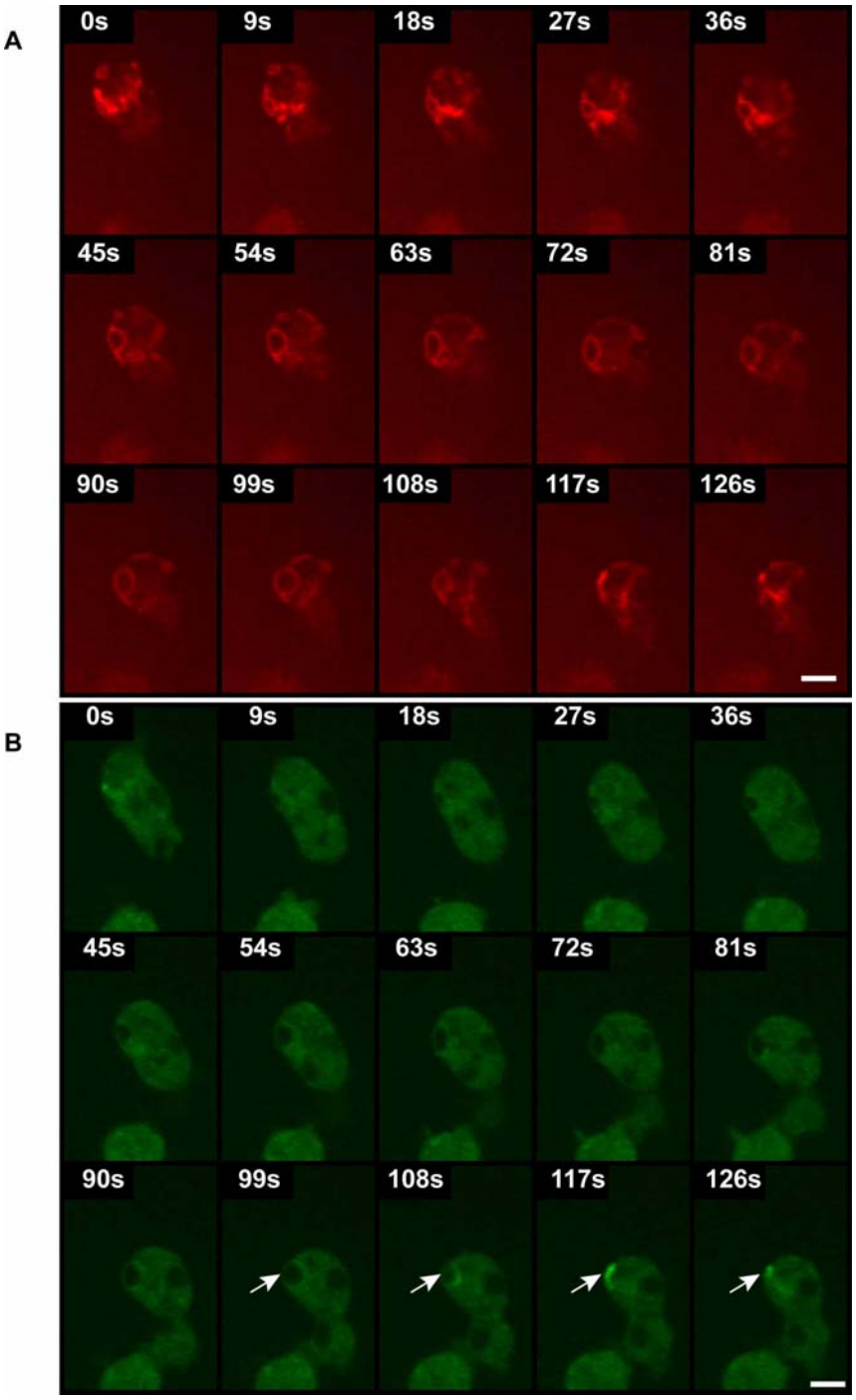

Figure 14:
LvsA localizes to CV membrane at late discharge stage. (A&B) The localization of RFP-Dajumin (A) and GFP-LvsA (B) in Ax2 cells under hypotonic stress. Pictures were taken at the same time for both colors. Arrows indicate the time frames of LvsA association with CV bladders. Scale bar, 5μm.

initiated (Figure 6E). In agreement with previous reports [30], I found that GFP-LvsA translocates to the CV membrane only at the discharge stage, and the period during which LvsA was associated with CVs prior to vacuole-plasma membrane fusion was brief, 18±5 seconds (n=30 cells) (Figure 14B). Surprisingly, LvsD did not localize to CV membranes (Figure 15A) and was always cytosolic, whether the cells were in isotonic or hypotonic medium and in all cell lines tested (data not shown).

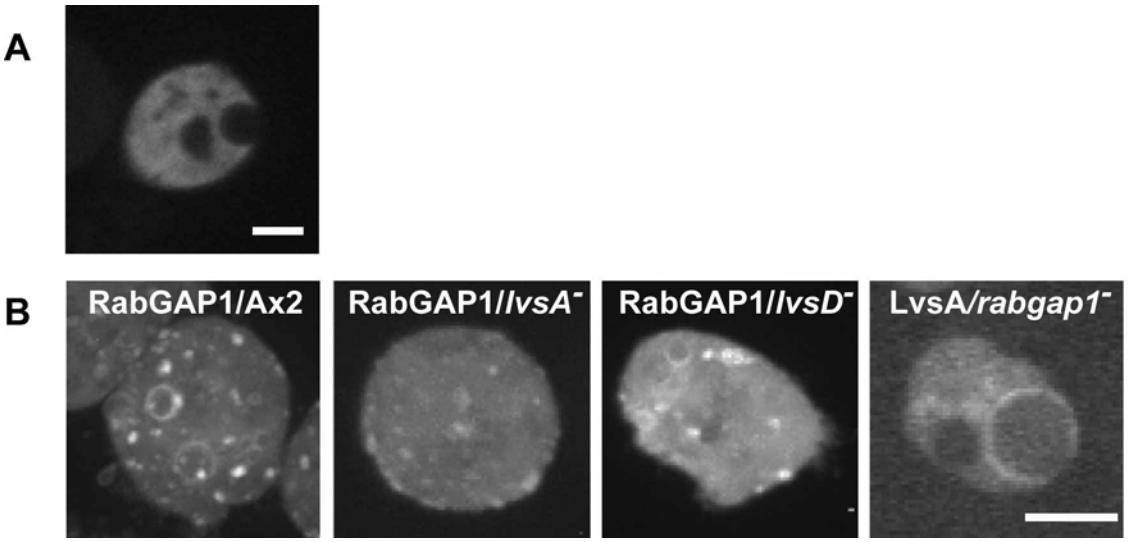

Figure 15:
Genetic interaction of LvsA, LvsD, and RabGAP1. (A) Localization of LvsD in Ax2 cells. (B) Localization of GFP-RabGAP1 in different cell lines and localization of LvsA in *rabgap1*$^{-}$ cells.

To further understand the epistatic relationships between LvsA, LvsD, and RabGAP1, I examined RabGAP1 localization in different *lvsA* and *lvsD* strains. In *lvsA*$^{-}$ cells, RabGAP1 localized to some punctate structures close to the bottom of the cells and on the plasma membrane (Figure 15B). Co-expressing GFP-RabGAP1 with

RFP-Dajumin confirmed that these were CV structures (data not shown). The fact that RabGAP1 only localized to CV to initiate the discharging stage suggested that the aberrant CV structures in *lvsA*$^{-}$ cells were the remnants of CVs that stopped growing after the discharging stage rather than the precursors of new CVs. RabGAP1 localization in *lvsD*$^{-}$ cells was similar to that in wild-type cells (Figure 15B), suggesting LvsD did not regulate RabGAP1 localization. In *rabgap1*$^{-}$ cells, LvsA still localized to CV bladders, which indicated that RabGAP1 was not required for LvsA CV membrane localization (Figure 15B).

RabGAP1-interacting Proteins

Although RabGAP1 was identified from a yeast two-hybrid screen using ERK1 as bait, I was unable to detect any *in vivo* interaction between RabGAP1 and ERK1 (data not shown). To identify possible regulators and effectors of RabGAP1, I purified a RabGAP1-containing complex from cells and analyzed it by mass spectrometry (Table 2; see Materials and Methods). None of the proteins discussed above were identified in the RabGAP1 complex, but several potential binding proteins were identified (Table 2). The most abundant peptides were from the SKP1 orthologues FpaA and FpaB, components of the SCF ubiquination complex. This result was not unexpected, as RabGAP1 contains an F-box domain, which often but not exclusively binds to a SKP to mediate the interaction between ubiquitin-E3-ligase and its substrate [110]. I performed co-immunoprecipitation

experiments and confirmed the *in vivo* interaction of RabGAP1, FpaA, and FpaB in an F-box domain-dependent manner (Figure 16).

Table 2:
Mass spectrometry analysis of the RabGAP1 complex
The RabGAP1-containing complex was immunoprecipitated and analyzed by mass spectrometry to determine the RabGAP1-interacting proteins. Wild-type Ax2 cells were used as a control for the RabGAP1/*rabgap1*$^{-}$ and RabGAP1^{R515A} /*rabgap1*$^{-}$ cells. Proteins that are uniquely identified in the RabGAP1/*rabgap1*$^{-}$ and/or RabGAP1^{R515A}/*rabgap1*$^{-}$ cells were listed in the table. Both spectra count (upper number in column 1-3) and total chromatogram intensity (lower number in column 1-3) were listed for each protein in each sample. The total number of identified distinct peptides (last column) was also listed for each protein.

Ax2	RabGAP1 /*rabgap1*$^{-}$	RabGAP1^{R515A} /*rabgap1*$^{-}$	Protein MW (Da)	protein	Distinct Peptides (#)
0 0.00E+00	50 8.01E+07	52 2.27E+08	80278.8	RabGAP1	12
0 0.00E+00	20 1.16E+07	9 9.31E+06	18718.3	FpaA	7
0 0.00E+00	17 8.50E+06	5 7.52E+06	18702.3	FpaB	7
0 0.00E+00	17 8.50E+06	5 7.52E+06	18702.3	FpaB copy	7
0 0.00E+00	4 1.74E+06	5 2.27E+06	42821.2	ubqA	4
0 0.00E+00	4 1.74E+06	5 2.27E+06	42777.2	polyubiquitin	4
0 0.00E+00	5 2.18E+06	4 1.81E+06	42730.2	ubqG	4
0 0.00E+00	4 1.74E+06	4 1.81E+06	34211.3	polyubiquitin	4
0 0.00E+00	4 1.74E+06	4 1.81E+06	34211.3	polyubiquitin	4
0 0.00E+00	3 1.28E+06	4 4.17E+06	17448.6	ubqC	4
0 0.00E+00	3 1.28E+06	4 4.17E+06	14671.4	ubqB	4
0 0.00E+00	3 1.18E+06	0 0.00E+00	68201.5	vatA	3

I do not know if RabGAP1 is a substrate for an SCF complex or may function as

an adaptor to associate a potential interaction with the SCF complex, targeting it for ubiquitination. I identified ubiquitin in the complex, but I did not observe any ubiquitination of immunoprecipitated, tagged RabGAP1 in wild-type cells, using an anti-ubiquitin antibody, or in wild-type cells co-expressing myc-ubiquitin using an anti-myc antibody. I cannot distinguish between the possibilities that RabGAP1 is ubiquitinated but rapidly degraded or that it is not ubiquitinated (see Discussion).

The V-ATPase A subunit, VatA, which also localized to CVs, was identified in the complex (Table 2). I do not know if RabGAP1 directly interacts with VatA or if the interaction is indirect (Table 2).

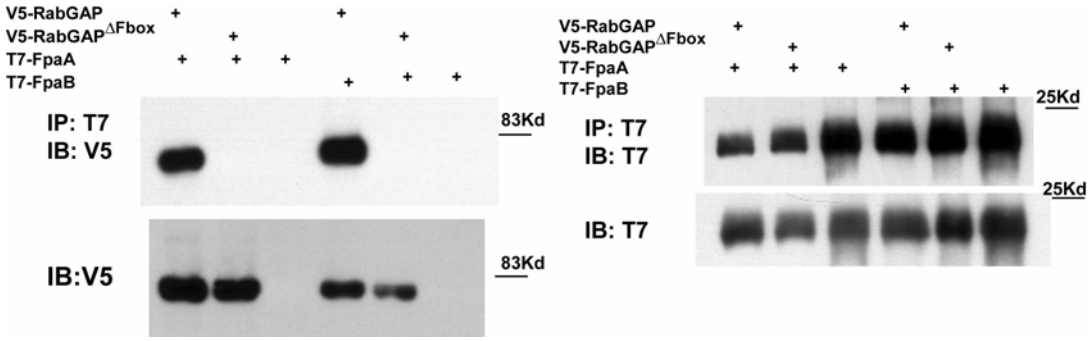

Figure 16:
Interaction of RabGAP1 and FpaA/FpaB in an F-box-dependent manner. The cell lysates from cells co-expressing with T7-FpaA or T7-FpaB and v5-RabGAP1 or v5-RabGAP1$^{\Delta Fbox}$ were immunoprecipitated with anti-v5 antibody and the Western blot was probed with either anti-T7 or anti-v5 antibody

RabGAP1, LvsA, and LvsD Regulate F-actin Polymerization and Chemotaxis

During my studies, I found that RabGAP1 was involved in not only CV regulation,

but also F-actin polymerization, and chemotaxis. In wild-type cells, the F-actin polymerized very rapidly upon cAMP stimulation, in ~5 seconds and up to 3-4 fold as measured by the actin amount in the Triton-insoluble fraction. A second peak occurring around 1 minute was much broader than the first one (Figure 17A). In *rabgap1*$^{-}$ cells, the F-actin polymerization upon cAMP stimulation was considerably higher than that in wild-type cells for both the first and second peaks (Figure 17A). Expressing RabGAP1 in *rabgap1*$^{-}$ cells complemented this phenotype. However, expressing the RabGAP1 abolishing the GAP activity (RabGAP1^{R515A}, RabGAP1^{Q551A}) or the one lacking the F-box domain (RabGAP1$^{\Delta Fbox}$) did not rescue this phenotype in *rabgap1*$^{-}$ cells, suggesting that the regulation of F-actin polymerization by RabGAP1 is F-box- and GAP activity-dependent (Figure 17A).

Interestingly, LvsA suppressed both the *rabgap1*$^{-}$ large CV phenotype and the higher F-actin polymerization of *rabgap1*$^{-}$ cells. The F-actin polymerization was greatly reduced in *lvsA*$^{-}$*/rabgap1*$^{-}$ cells, only half of that in wild-type cells for both peaks (Figure 17B). The Myosin II assembly was also reduced in *lvsA*$^{-}$*/rabgap1*$^{-}$ cells (Figure 17B). *lvsA*$^{-}$ cells and all of the other *lvsA*$^{-}$ strains, such as *lvsA*$^{-}$*/lvsD*$^{-}$ and *lvsA*$^{-}$*/lvsD*$^{-}$*/rabgap1*$^{-}$, exhibited lower F-actin polymerization and Myosin II assembly (Figures 14B). All of the *lvsA null* strains I examined exhibited similar phenotypes including aberrant CV structures, phagocytosis defects, cytokinesis defects, (data not shown), and aberrant responses to hypotonic stress (Table 1), lower F-actin polymerization, and lower Myosin

II assembly (Figures 14B), suggesting that all of the phenotypes were due to disrupting the *lvsA* gene. Although LvsA^{OE} cells exhibited normal F-actin polymerization (Figure 17D; data not shown), the F-actin polymerization was lower in LvsA^{OE}/*rabgap1*$^{-}$ cells than in wild-type cells (Figure 17D).

lvsD^{-} cells exhibited higher F-actin polymerization, as observed in *rabgap1*$^{-}$ cells. However, in *lvsD*$^{-}$/*rabgap1*$^{-}$ cells, the F-actin polymerization was greatly reduced, lower than wild-type cells and similar to that of *lvsA*^{OE}/*rabgap1*$^{-}$ cells (Figure 17C).

Since polymerization of F-actin in the leading edge drove pseudopodia protrusion during chemotaxis, I was not surprised that *rabgap1*$^{-}$ cells exhibited a more elongated shape during chemotaxis and moved faster than wild-type cells (Figure 18; Table 3). The difference could only be detected under low cell density conditions but not under regular condition (data not shown). Consistent with lower F-actin polymerization and Myosin II assembly, all of the cell lines disrupting the *lvsA* gene exhibited chemotaxis defects: cells were round and moved slowly (Figure 18; Table 3; data not shown).

Figure 17:
RabGAP1, LvsA, and LvsD regulate F-actin polymerization. Chemoattractant stimulated F-actin polymerization as described in the Experimental Procedures (A, B, C, D). Chemoattractant stimulated Myosin II assembly as described in the Experimental Procedures (B).

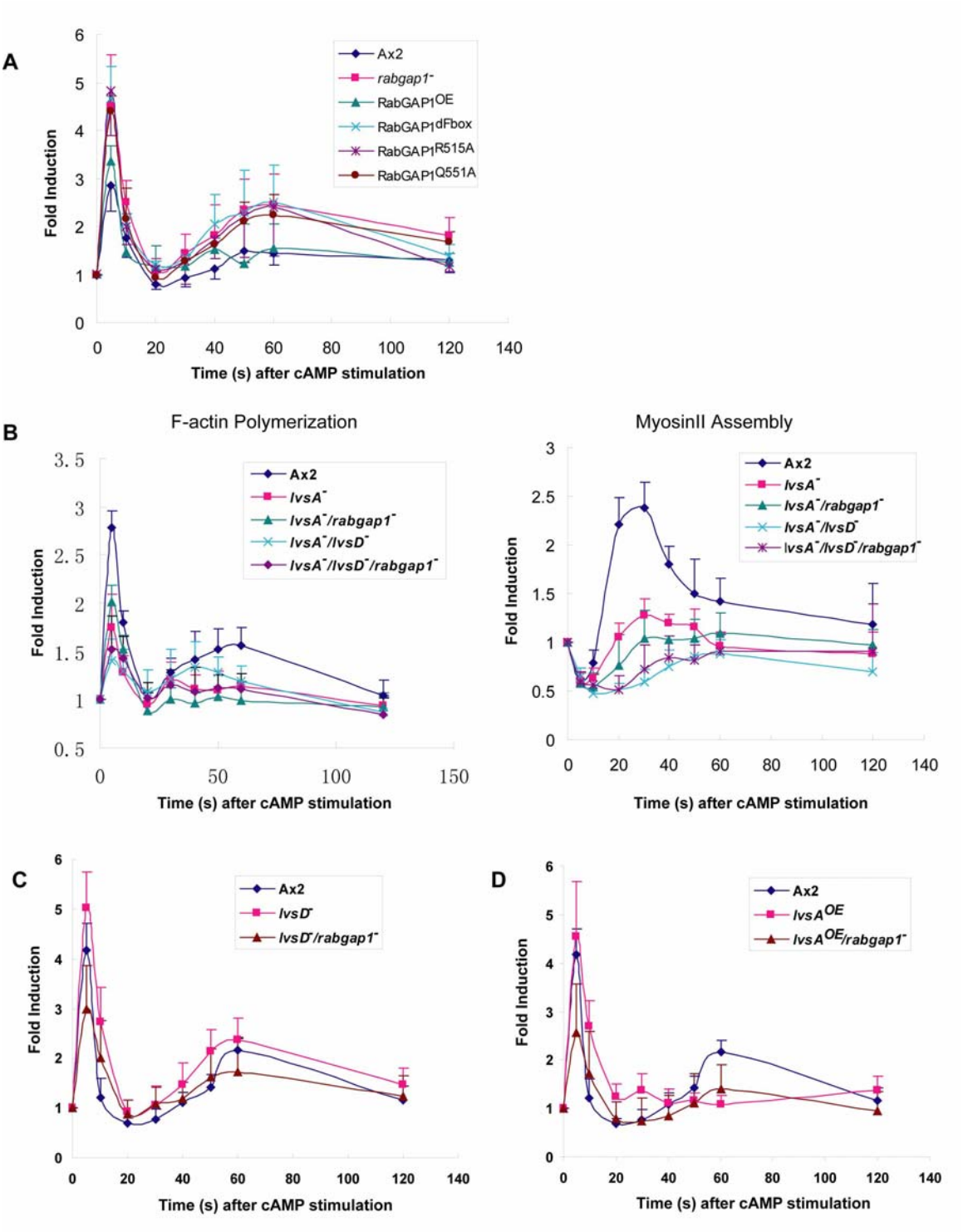
A
Fold Induction
Time (s) after cAMP stimulation
Ax2
rabgap1-
RabGAP1OE
RabGAP1dFbox
RabGAP1R515A
RabGAP1Q551A
B
F-actin Polymerization
MyosinII Assembly
Fold Induction
Time (s) after cAMP stimulation
Ax2
lvsA-
lvsA-/rabgap1-
lvsA-/lvsD-
lvsA-/lvsD-/rabgap1-
C
Fold Induction
Time (s) after cAMP stimulation
Ax2
lvsD-
lvsD-/rabgap1-
D
Fold Induction
Time (s) after cAMP stimulation
Ax2
lvsAOE
lvsAOE/rabgap1-

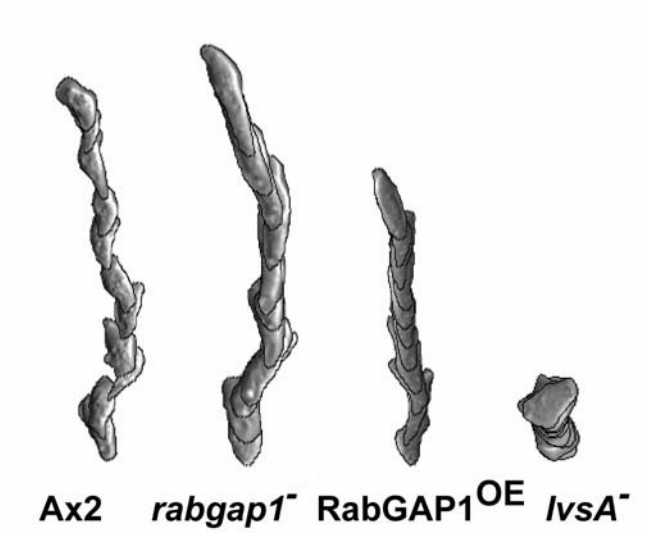

Figure 18:
RabGAP1 and LvsA regulate chemotaxis. Representative traces of wild-type Ax2, *rabgap1*$^{-}$, *lvsA*$^{-}$, and RabGAP1 overexpression in *rabgap*$^{-}$ cells moving up a gradient towards a micropipette filled with a chemoattractant. Time-lapse recordings were taken at 6-second intervals; superimposed images show the cells' shape, direction, and length of path at 1-minute intervals.

Table 3:
DIAS analysis of chemotaxis. Numbers are mean values±standard deviation. Speed indicates speed of the cell's centroid movement along the total path. Direction change is a relative measure of the number and frequency of turns the cell makes. Larger numbers indicate more turns and less efficient chemotaxis. Directionality is a measure of the linearity of the pathway. Cells moving in a straight line to the needle have a directionality of 1.00. Roundness is an indication of the polarity of the cells. Larger numbers indicate the cells are more round and less polarized.

Strain	Speed (mm/min)	Directional change (deg)	Roundness (%)	Directionality
Ax2	10.7±2.9	57.7±6.5	68.9±4.0	0.68±0.14
rabgap1^{-}	12.1±0.3	72.9±4.0	54.5±1.0	0.50±0.01
RabGAP1^{OE}	8.1±1.5	61.0±3.6	54.6±2.0	0.75±0.04
lvsA^{-}	3.7±1.0	68.9±5.8	82.7±7.5	0.13±0.07

DISCUSSION AND ANALYSIS

The Regulation of CV Activity

I provide evidence that RabGAP1 regulates CV formation and activity in *Dictyostelium* and is specifically required for discharging the CV by regulating the fusion of the CV with the plasma membrane. I demonstrate that RabGAP1 associated with the CV during the late charging stage prior to the CV/plasma membrane fusion, and I determined that *rabgap1*$^{-}$ cells were unable to effectively discharge the CV by fusing to the plasma membrane. Under hypotonic conditions, the swollen CV bladders pushed the plasma membrane out, forming a bleb, whereupon some of the bladder contents were released. As soon as some of the content was released from the bladder, the bladder retracted, although the discharge was not complete. These observations suggest that membrane tension may be involved with water release in the absence of efficient CV/plasma membrane fusion mediated by RabGAP1. I suggest that, as the CV bladders charge, they are driven against the plasma membrane, forming blebs in the absence of RabGAP1. This tension may cause a localized, small rupture in the plasma membrane allowing the release of the CV contents. Once some of the content is released, membrane tension is reduced and the cell reseals the gap in the CV and plasma membranes. Such a resealing process was previously described by Gerisch and colleagues [31]. Using a fine glass needle to perforate the top of the bladder, the contents of the punctured vacuoles were released and the cells survived. However, the cells lysed immediately by punching

other parts of the plasma membrane [31]. I postulate that there are at least two forces to drive CV discharge: membrane tension and CV/plasma membrane fusion driven by the RabGAP1 pathway. The former is not the major force mediating discharge in wild-type cells since, in the absence of RabGAP1, the discharging is inefficient in that it takes longer and some content remains in the bladders. Under isotonic conditions, CV discharge may not occur often and discharge is not critical for the cell's survival. In the absence of RabGAP1, CV/plasma membrane fusion is blocked and large vesicles accumulate. This finding suggests that the RabGAP1 pathway is the major pathway regulating CV discharge. With the strong phenotype, *rabgap1*$^{-}$ cells provide a good model to study membrane fusion.

Both Drainin and RabGAP1 contain a TBC domain and, like RabGAP1, disrupting Drainin results in large CV bladders and abnormal CV discharge. My data suggest that RabGAP1 and Drainin are not redundant. Instead, RabGAP1 lies downstream of Drainin to regulate CV discharge because RabGAP1 suppresses the *drainin*$^{-}$ large vacuole phenotype but not *vice versa* and Drainin is recruited to the CV membrane prior to RabGAP1. *drainin*$^{-}$ cells exhibit a more severe phenotype than *rabgap1*$^{-}$ cells, as the average vacuole size is larger, and *drainin*$^{-}$ cells are sensitive to hypotonic stress while *rabgap1*$^{-}$ cells are not. *rabgap1*$^{-}$ cells can discharge in an atypical manner, which also occurs in some of the *drainin*$^{-}$ cells. Expressing RabGAP1 in *drainin*$^{-}$ cells significantly reduces but does not eliminate this type of discharge, suggesting these

two proteins regulate different steps in this pathway. I suggest that RabGAP1's major function is to mediate vacuole/plasma membrane fusion and that Drainin functions, but is not essential, in this RabGAP1-mediated pathway. As I mentioned above, there are at least two forces driving the CV discharge in *Dictyostelium*, membrane tension and fusion of the CV/plasma membrane mediated by RabGAP1. In *drainin*$^{-}$ cells, the membrane tension still exists since the bladders still round up before discharge. The RabGAP1 pathway is impaired, as the *rabgap1*$^{-}$ type abnormal discharge occurs in *drainin*$^{-}$ cells. Since RabGAP1 still localizes to the CV membrane, other regulators must exist.

The localization of RabGAP1 to the membrane of the CV is necessary for its proper function. Without the two membrane binding motifs, the 382-452 region and the 9 hydrophobic residue stretch, RabGAP1 no longer localized to CV membrane and did not rescue the null phenotype. Furthermore, RabGAP1$^{\Delta 9}$ had a dominant-negative effect in Ax2 cells, suggesting without the 9 hydrophobic region, RabGAP1 still interacted with its substrates but not in the right place and could not function normally. There is an 8 hydrophobic residue stretch inside the TBC domain of Drainin which is required for its membrane localization [31]. My sequence analysis reveals that other TBC domain-containing proteins have similar motifs which might be universal membrane localization motifs of TBC domain-containing proteins.

RabGAP activity is required for RabGAP1 function, as RabGAP1^{R515A} or RabGAP1^{Q551A}, carrying mutations in the dual fingers, did not rescue the large vacuole

phenotype in *rabgap1*$^{-}$ cells. Expression of either mutant RabGAP1 in wild-type cells resulted in a dominant negative effect causing large vacuoles. Furthermore, expression of RabGAP1^{R515A} or RabGAP1^{Q551A} in *rabgap1*$^{-}$ cells led to a more severe discharge defect in which the RabGAP1 associated with CV bladders continuously for 5 minutes without discharge. Normally, the mutations in catalytic residues would not change the substrate specificity. Thus, RabGAP1^{R515A} or RabGAP1^{Q551A} should still bind with the same substrate as wild-type RabGAP1 does. But these two mutations resulted in enlarged vacuoles in *rabgap1*$^{-}$ cells, indicating the complete depletion of the substrates. This finding suggests the existence of another RabGAP sharing the same substrate with RabGAP1. In *rabgap1*$^{-}$ cells, the RabGAP de-activates the Rab, but not efficiently, and the cells develop the large vacuole phenotype. When I expressed RabGAP1^{R515A} or RabGAP1^{Q551A} in *rabgap1*$^{-}$ cells, all of the Rabs regulated by these two RabGAPs appeared in the constitutively activated form which causes a more severe phenotype with larger vacuoles. Another possible explanation of these observations is that in *rabgap1*$^{-}$ cells, the intrinsic GTPase activity of Rabs still exists. RabGAP1^{R515A} or RabGAP1^{Q551A} would bind with Rabs and inhibit their internal GTPase activity, leading to the dominant-negative phenotypes.

Since RabGAP activity is required for RabGAP1 function in both vacuole formation and F-actin polymerization, I expect that some of the phenotypes of *rabgap1*$^{-}$ cells result from a specific Rab GTPase trapped in the GTP-bound form for an extended

time. My findings indicate that Rab11A and Rab8A both function in the RabGAP1 pathway, because overexpression of either rescued the large vacuole phenotype but not other Rabs (of those tested) and both interacted *in vitro* with RabGAP1. I demonstrate that Rab8A localized to the CV bladders and exhibited the same pattern of subcellular localization as RabGAP1, co-localizing with RabGAP1 during the late charging stage with similar timing. RabGAP1 was not required for the Rab8A localization since Rab8A still localized to the CV membrane in *rabgap1*$^{-}$ cells. As I have been unable to generate a Rab8A knockout, I could not test a dependency for RabGAP1's localization on Rab8A.

Rab11A, like Dajumin, was found exclusively associated with the CV and cells expressing dominant-negative Rab11A (Rab11A^{N125I}) were sensitive to hypotonic stress, consistent with a Rab11A being required for CV discharging [27]. The Bush group also found that Rab11A no longer localized to CV and exhibited a diffuse punctate pattern along with the cell surface in hypotonic conditions. My studies indicate that Rab11A remains associated with the CV membranes under hypotonic conditions during both the charging and discharging stages.

If Rab8A and Rab11A are regulated by RabGAP1 and inactivated, I expect constitutively active Rab8A or Rab11A to exhibit the same large vacuole phenotype as observed in *rabgap1*$^{-}$ cells. However, I did not observe enlarged CV bladders when I overexpressed Rab8A^{ca}, Rab11A^{ca}, or both in wild-type cells. RabGAP1 may regulate other Rabs and/or RabGAP1 may have other functions independent of its GAP activity

that are required for proper CV discharge, possibly acting as a Rab effector.

Although Rab14 did not co-localize with RabGAP1 and interact with RabGAP1 in the pull-down assay, I could not rule out the possibility that Rab14 was involved in the RabGAP1 pathway. From the same yeast two-hybrid screen using ERK1 as bait, Rab14 was also identified (data not shown). *In vitro* GAP assays of Rab8A, Rab11A, and Rab14 are critical experiments for determining whether any of these Rabs are the genuine substrates of RabGAP1. Unfortunately, I was unable to purify RabGAP1 and perform the assays.

Drainin lacks the conserved catalytic Arg and Gln thought to be required for Rab GAP activity [111]. Mutation of either of these in *bona fide* Rab GAPs leads to loss of activity. Therefore, I suggest that Drainin lacks GAP activity. However, as overexpression of Rab8A rescues both the large vacuole phenotype and the abnormal discharge in *drainin*$^-$ cells, I suggest that Rab8A and Drainin may interact directly or genetically in the same pathway and the *drainin*$^-$ phenotype may be caused by mis-regulation of Rab8A. Drainin might represent a new class of TBC domain-containing protein which lacks RabGAP activity but is involved in Rab signaling. An alternative possibility is that Drainin may not directly regulate Rabs, but may function similarly to TRE2, a TBC domain-containing protein lacking the conserved Arg and Gln residues, which binds to and activates Arf6 [112]. In HT1080 cells, Rab8 mediates membrane protrusions and is functionally linked with Arf6 and co-localizes with Rab11 [113]. Thus, Drainin may

function like TRE2 in regulating Arf and, through an Arf-mediated pathway, may control Rab8A and possibly Rab11 to mediate CV size and function.

Expression of RabGAP1 lacking the F-box results in a smaller vacuole phenotype and it would not complement the high F-actin polymerization in *rabgap1*$^{-}$ cells, but the function of the F-box is still unclear. I found two *Dictyostelium* SKP1 orthologues in RabGAP1-containing complexes that interact with RabGAP1 in an F-box-dependent manner. Both the F-box-containing proteins and the SKP proteins are components of the SCF (Skp-cullin-F-box) ubiquitin E3-ligase complex. The substrate specificity is conferred by a Skp adaptor and an F-box protein. Usually, F-box proteins contain another domain for protein-protein interaction and the most common ones are WD40 repeats and leucine-rich repeats [110, 114]. I expect that RabGAP1 is either a target of ubiquitination or functions as an adaptor to bring another protein to the SCF complex, which is then ubiquitinated. I do not have direct evidence for either model and I was unable to detect RabGAP1 ubiquitination, possibly because the steady-state level of ubiquitinated RabGAP1 is very low in cells under my assay conditions. Alternatively, the RabGAP1 F-box may not mediate the interaction RabGAP1 with an ubiquitin-E3-ligase complex but may mediate the formation of a non-SCF-containing complex lacking ubiquitin ligase activity such as Mfb1p, Ctf13, and Rcy1p [115-118]. Those proteins interact with Skp proteins in an F-box-dependent manner but not with the other components of the SCF complex to play their cellular roles.

The CV system is the osmoregulatory organelle of free-living amoebae and protozoa. It is interesting to know if such a distinct compartment exists in eukaryotic cells. The CV system is a post-Golgi compartment, as determined by the presence of O-glycosylated proteins in its membranes [19]. My and previous studies demonstrate that at least 3 Rabs localize to the CV system in *Dictyostelium*, Rab8A, Rab11A, and Rab14 [27, 32]. Rab8 is involved in secretory vesicular traffic between the TGN and the plasma membrane in mammalian cells [119]. Rab11 localizes to both recycling endosomes and the Golgi to regulate the traffic between the trans-golgi network-to-plasma membrane in epithelial cells [120]. Mammalian Rab14 localizes to the Golgi/TGN and to early endosomes and cycles between early endosomes and the Golgi cisternae [121, 122]. A recent paper suggested both Rab8 and Rab11 partially co-localize on some vesicles in HT1080 fibrosarcoma cells [113]. Rab8 but not Rab11 localizes to a special tubular compartment which is convertible with the vesicles in at least 3 cell lines. The tubular structure is extended to cell protrusion to regulate the recycling of the membrane to mediate the protrusion formation [113]. This special compartment to recycle the membrane is similar to the CV in *Dictyostelium* in that both Rab8 and Rab11 localize to these compartments and both compartments consist of vacuolar and tubular structures which are interconvertible. Furthermore, both compartments are connected with the plasma membrane and the trafficking of the compartments is dynamics. Lastly, these two compartments are involved in transportation to the cell surface. The special

tubular-vacuolar structures which Rab8 localizes to transport membrane and probably some other molecules as well. The CV system is involved in a non-classical means of transporting DdCAD-1 to the cell surface [20]. It would be interesting to know if these two compartments are evolutionary conserved.

The Regulation of BEACH Proteins

A second site suppressor screen identified two BEACH proteins, LvsA and LvsD, that genetically interact with RabGAP1 in controlling CV morphology and function. BEACH proteins contain highly conserved domains and several have been linked to human diseases (i.e. LYST, LRBA, and neurobeachin) [37, 38, 123, 124]. The *lyst* gene, the first BEACH gene identified, is deleted or has a frame-shift mutation in Chediak-Higashi syndrome (CHS) patients or in beige mice leading to oculocutaneous albinism, easy bruisability, and bleeding as a result of deficient platelet dense bodies, severe immunodeficiency, and peripheral neuropathy [37, 38]. LRBA is overexpressed in several cancers and the overexpression of LRBA facilitates cancer cell growth [123, 124]. The neurobeachin gene is disrupted in a patient with idiopathic autism [124]. Although the BEACH proteins are important, little is known about their function and molecular mechanisms, mainly because BEACH proteins are large proteins and majority are over 400 kD. *Dictyostelium* is the only unicellular model system that has the full sets of BEACH proteins found in metazoans [45]. It is a robust system in which to study

BEACH protein function because of the availability of genetic and biochemistry analyses.

My studies indicate that LvsA and LvsD play opposite roles in CV regulation in *Dictyostelium*. *rabgap1*$^{-}$ cells overexpressing LvsA and *lvsD*$^{-}$/*rabgap1*$^{-}$ form vacuoles that are even larger than those observed in *rabgap1*$^{-}$ cells, whereas disrupting LvsA or overexpressing LvsD rescues the large vacuole *rabgap1*$^{-}$ phenotype. Because LvsA and LvsD have opposite effects in a *rabgap1*$^{-}$ background, and given the localization of these two proteins, I speculate that LvsD may interact with LvsA in the cytosol and release it under hypo-osmotic conditions to fulfill the regulation of the CV. I tested these possibilities using co-immunoprecipitation. Since both LvsA and LvsD are large proteins, 408 kD and 317 kD respectively, I experienced difficulty in detecting a reasonable amount of proteins. I used the C-termini of LvsA and LvsD, including the PH-like domain, the BEACH domain, and the WD-40 domain, which are the potential interacting domains. Although I detected the interaction of C-termini of LvsA and LvsD, the interaction was not specific since I could also detect co-immunoprecipitation of C-termini of LvsB with LvsA or LvsD. Furthermore, by employing mass spectrometry analysis of complexes using tagged C-termini, no interactions were identified. Therefore, the proteins may not form a complex or the amount of that complex may be too low to be detected in my assays. Another possibility is that the truncated BEACH proteins are both nonfunctional [30] and defective in binding to the regulators or effectors. I cannot

exclude the possibility of heterodimer formation. The Tong group [47] demonstrated the interaction of two molecules of the BEACH protein, Neurobeachin. Usually, the large proteins function as scaffold proteins. Possibly, these two proteins compete for the same binding proteins. This is the first demonstration that two BEACH proteins play opposite roles in regulating same physiological process. The antagonistic function between BEACH proteins like LvsA and LvsD might shed light on the general regulation of BEACH proteins. Although the classification of BEACH proteins [51] suggests LvsD belongs to Class V, which is *Dictyostelium* and *Arabidopsis* specific, Class V is closely related to Class IV, which has several human orthologues.

I and Wu et al [30] found that LvsA is required for the integrity of the CV system and possibly the discharge of the CV. LvsA associates with the CV membrane at the late discharge stage and can be briefly observed in a "patch" of CV membrane that remains at the plasma membrane after fusion. Shortly after fusion, LvsA and other late stage CV proteins (RabGAP1, Rab8A, and Drainin) dissociate with the membrane structure while Dajumin and Rab11 remain in the patch. It has been suggested that the discharge of the CV is a "kiss and run" event but the recycling of the CV membrane might occur [17]. Indirect evidence of recycling exists: newly formed bladders frequently generate from the sites of CV-plasma membrane fusion [16, 17, 19]. Furthermore, cells lacking clathrin or the clathrin assembly proteins AP1 (*apm1*$^{-}$) and AP180 are hypo-osmotic sensitive and *clathrin*$^{-}$ cells and *apm1*$^{-}$ cells cannot assemble intact CV structures, suggesting a

clathrin-mediated recycling of CV components is required for CV formation [125-127]. RabGAP1, in addition to V-ATPase and Dajumin, co-localizes to the punctate structures in *lvsA*$^{-}$ cells. As RabGAP1 only associates with the CV membrane at the discharge stage, these findings suggest that the punctate structures are CVs that cannot re-assemble after discharging. I suggest that LvsA maintains the integrity of the CV by regulating or functioning in the recycling of the CVs rather than the biogenesis.

Presently, I do not know if LvsA is required for CV discharging since *lvsA*$^{-}$ cells lack normal CV structures. However, LvsA^{OE} cells exhibit normal CV discharging, consistent with a model in which LvsA controls CV recycling and new CV formation and not CV charging or discharging. The suppression of the large vacuole phenotype in *rabgap1*$^{-}$ cells by disruption of LvsA is therefore caused by the requirement of LvsA for normal CV formation. RabGAP1 is not required for LvsA association with the CV immediately prior to discharge.

Both the RabGAP1 pathway and the LvsA and LvsD pathways regulate CV activity, but with different timing. RabGAP1 is not required for the CV localization of LvsA, and LvsA is probably not recruited by a Rab directly since it is shown that LvsA binds to membranes in a GTP-independent manner *in vitro* [30]. Although I do not have direct evidence that RabGAP1 and LvsA and LvsD function in the same pathway, LvsA and LvsD act as a suppressor and an enhancer of the *rabgap1*$^{-}$ large CV phenotype. The connection between BEACH proteins and the RabGAP1 protein strongly suggests that

BEACH proteins and Rab proteins might function together to play their cellular roles. Another BEACH protein, Bchs, antagonizes Rab11 in synapse morphogenesis in *Drosophila* [128]. A recent paper found genetic interactions between Bchs and another Rab, Rab-RP1 and, most importantly, the Ubiquitin pathway [129]. Considering that RabGAP1 contains an F-box domain, the regulation of BEACH proteins by Rabs and the Ubiquitin pathway might be a generalization in all eukaryotic cells. There is still much to learn about the regulation of CV activity by BEACH proteins. What recruits LvsA to the CV and how does LvsA regulate the formation of the CV in *Dictyostelium*?

In light of my and published data, I propose a model of CV biogenesis and function in *Dictyostelium* (Figure 19A). Under isotonic conditions, the CV is not very active and RabGAP1, LvsA, LvsD, Drainin, and Rab8A are predominantly cytosolic. Dajumin and Rab11A are always associated with the CV tubular and vacuolar structures, although Dajumin is not required for CV biogenesis [19]. Upon hypotonic stress, the CVs start collecting water. Late in this process, in separate and independent steps, Drainin is recruited to the CV membrane followed by RabGAP1 and Rab8A, whereupon the vesicles appear to stop charging. Shortly before CV/plasma membrane fusion, LvsA is recruited to the vacuoles. The vacuoles then fuse with the plasma membrane and discharge their contents. Rab8A, RabGAP1, Drainin, and LvsA dissociate from the plasma membrane and the next charging begins (Figure 19B). LvsA is required for the integrity of the CV complex; the cells in which *lvsA* is disrupted lack an intact CV system

and these cells lyse in hypotonic medium (Figure 19C). *rabgap1*$^{-}$ cells have enlarged vacuoles resulting from a blockage in CV/plasma membrane fusion. Under hypotonic conditions, *rabgap1*$^{-}$ cells discharge but without fusion (Figure 19D).

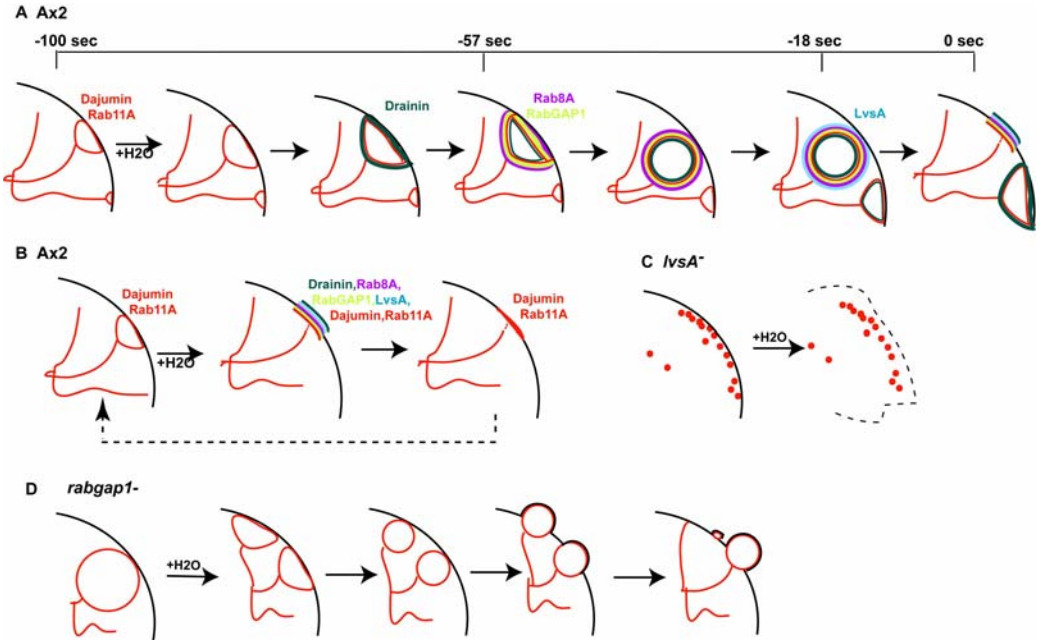

Figure 19:

Model of the RabGAP1 pathway. (A) CV activity in *Dictyostelium* cells. The CV system can be visualized using Dajumin which is labeled as red. Under isotonic conditions, the CV is not very active. RabGAP1, LvsA, LvsD, Drainin, and Rab8A are predominantly cytosolic. Rab11A has localization similar to that of Dajumin, and association of both the tubular and vacuolar structures of CV complex. Once cells are under hypotonic stress, the tubules of the CVs start collecting water. When the size of the CVs reaches a certain range, Drainin is recruited to the CV membrane. Rab8A and RabGAP1 are then recruited to the CV membrane to stop the further fusion of the CV. Through an unknown mechanism, LvsA is recruited to the membrane of CVs. The discharge of the CVs and fusion with the plasma membrane occur right after the LvsA recruitment. (B) After discharging, Dajumin and Rab11A still associate with plasma membrane. Rab8A, RabGAP1, and LvsA dissociate from plasma membrane. Another cycle of charging starts. (C) The cells disrupting the *lvsA* gene lack an intact CV system. Those cells only have punctate structures which might be the remnants of the CV system. Under hypotonic stress, cells lyse. (D) *rabgap1*$^{-}$ cells have enlarged vacuoles because of aberrant fusion of the CVs to the plasma membrane. *rabgap1*$^{-}$ cells still discharge water but inefficiently.

Function of V-ATPase

V-ATPase is a conserved enzyme in all eukaryotic cells that transforms the energy from ATP hydrolysis to active transport H^+. In turn, the transmembrane electrochemical potential of H^+ is used to transport other ions or macromolecules across the membrane [25]. It was previously suggested that *Dictyostelium* V-ATPase, which predominantly localizes to the CV complex, establishes a proton gradient to transports other ions into CVs, resulting in an inward flux of water [16]. Here, I present data indicating that, after inhibiting V-ATPase activity of cells in isotonic medium, the CV still collects water and charges, but the cells lyse when placed in water, suggesting that V-ATPase is required for vacuole discharging but not charging [20]. Questions have been raised by this observation. What drives the accumulation of water in CV? What helps to maintain the water inside the water-permeable membrane? How does V-ATPase regulate discharge?

The cell morphological change after NBD-Cl treatment is similar to that in quinine treatment [130]. After treatment with quinine, cells form large CVs, develop elongated forms, and are less adhesive to the substratum [130]. It has been shown that quinine blocks the voltage-dependent K^+ channel which is found in a CV-enriched cell fraction [131]. It is possible that one of V-ATPase's functions is to regulate the voltage-dependent K^+ channel on the CV. However, in quinine-treated cells, CVs still discharge [130], suggesting the K^+ channel does not regulate discharge and is not the only

downstream event regulated by V-ATPase. There was a report of the existence of a Ca^{2+}/H^{+} antiport on the CV in *Dictyostelium*. The PH gradient generated by H^{+}-ATPase is used to pump Ca^{2+} into the CV [132]. The Ca^{2+} regulated pathway might be the one that regulates CV discharge.

CV, Ca^{2+}, and Chemotaxis

In *Dictyostelium*, there is debate whether Ca^{2+} is involved in chemotaxis. Stimulation with the chemoattractant cAMP leads to an influx of Ca^{2+} and elevation of cytosolic Ca^{2+} [78-80]. There are two intracellular Ca^{2+} storage mechanisms in *Dictyostelium*, the ER and the CV. The former is not required for the chemotaxis since loss of function of the InsP(3) receptor-like gene, *iplA*, does not result in any chemotaxis defect in *Dictyostelium* [86]. In this dissertation, I provide evidence that the CV regulators RabGAP1, LvsA, and LvsD are involved in F-actin polymerization and chemotaxis. It is strongly suggested that the CV is the major intracellular calcium source for chemotaxis and calcium is a messenger for chemotaxis. The regulation of chemotaxis by calcium probably takes place through the actin-binding proteins to regulate F-actin polymerization.

The chemotactic activity of CHS neutrophils is greatly impaired, probably due to the giant granules in the cells [133, 134]. In *Dictyostelium*, *lvsA*$^{-}$ cells exhibit lower F-actin polymerization, Myosin II assembly, and chemotactic activity, whereas *lvsD*$^{-}$ cells

exhibit higher F-actin polymerization, suggesting that LvsA and LvsD have opposite role in regulating actin polymerization. LvsA and LvsD act as a suppressor and an enhancer of the *rabgap1*$^{-}$ large vacuole phenotype. The evidence strongly suggests that LvsA and LvsD antagonize each other to control CV activity and regulate F-actin polymerization.

lvsA^{-} cells have a conditional cytokinesis defect which is a typical phenotype of cells with inactivated Myosin II, such as *mhcA*$^{-}$ and *mlckA*$^{-}$ [41, 135]. Consistently, in *lvsA*$^{-}$ cells the Myosin II assembly is greatly reduced compared to Ax2 cells. In *Dictyostelium*, Myosin II is regulated by essential myosin light chain and regulatory myosin light chain, which are Ca^{2+} binding proteins [136]. The cytokinesis defect and lower Myosin II assembly in *lvsA*$^{-}$ cells are probably due to the misregulation of Ca^{2+}.

There is increasing evidence that Rab proteins are involved in regulating cell migration by recruiting integrins and growth factor receptors by Rab4- and Rab11-driven pathways [102, 137]. Rab8A and Rab11A regulate membrane recycling back to the plasma membrane and lead to protrusion formation in mammalian cells [113, 138]. Here, I present evidence that RabGAP1 is involved in chemotaxis in *Dictyostelium,* possibly by controlling cytosolic Ca^{2+} concentration. This provides a new concept of how Rabs regulate cell migration. It was reported that constitutively activated Rab8A (Rab8A^{ca}) causes actin-rich membrane protrusions in vegetative *Dictyostelium* cells [64]. Since Rab8A suppresses the *rabgap1*$^{-}$ large vacuole phenotype and interacts with RabGAP1, it is possible that RabGAP1 regulates Rab8A to control the F-actin-polymerization in

Dictyostelium.

In conclusion, I identified the TBC domain-containing protein RabGAP1 which is involved in CV/plasma membrane fusion. I identified two membrane localization motifs in RabGAP1 which might be the general localization motifs for RabGAPs. Another TBC domain-containing protein, Drainin, when deleted, causes similar but more severe phenotypes than *rabgap1*$^-$ cells. Drainin is an upstream regulator of RabGAP1. Rab8A rescues the *drainin*$^-$ morphology and abnormal discharge phenotypes, whereas both Rab8A and Rab11A are involved in RabGAP1 pathway. By REMI screening, I identified LvsA and LvsD as a suppressor and an enhancer of the *rabgap1*$^-$ large vacuole phenotype. This is the first demonstration that two BEACH proteins antagonize and regulate the same process. LvsA maintains the CV's integrity, perhaps by regulating CV recycling. RabGAP1, LvsA, and LvsD regulate F-actin polymerization and chemotaxis, probably by regulating the Ca^{2+} concentration. My work helps to define CV formation and regulation. I identify a new function of the CV, which is to regulate F-actin polymerization and chemotaxis.

ACKNOWLEDGEMENTS

This chapter, in part, is material to be submitted for publication in 2007, by Fei Du, Kimberly Edwards, Zhouxin Shen, Binggang Sun, Steven Briggs, Arturo De Lozanne, and Richard A. Firtel. The dissertation author was the primary investigator and author of this paper. Co-author Kimberly Edwards performed REMI suppressor/enhancer screening with me and did co-immunoprecipitation of RabGAP1. Zhouxin Shen and Steven Briggs performed mass spectrometry analysis of the RabGAP1 complex. Binggang Sun did yeast two-hybrid screening using ERK1 as bait and identified the *rabgap1* gene. Arturo De Lozanne provided the LvsA knock-in, *drainin*$^-$ cell line and the anti-LvsA antibody. Co-author Richard A. Firtel supervised the work, in whole.

REFERENCES

1. Eichinger, L., et al., *The genome of the social amoeba Dictyostelium discoideum.* Nature, 2005. 435(7038): p. 43-57.

2. Hoeller, O. and R.R. Kay, *Chemotaxis in the absence of PIP3 gradients.* Curr Biol, 2007. 17(9): p. 813-7.

3. Dynes, J.L., et al., *LagC is required for cell-cell interactions that are essential for cell-type differentiation in Dictyostelium.* Genes Dev, 1994. 8(8): p. 948-58.

4. De Lozanne, A. and J.A. Spudich, *Disruption of the Dictyostelium myosin heavy chain gene by homologous recombination.* Science, 1987. 236(4805): p. 1086-91.

5. Klein, P.S., et al., *A chemoattractant receptor controls development in Dictyostelium discoideum.* Science, 1988. 241(4872): p. 1467-72.

6. Kumagai, A., et al., *Regulation and function of G alpha protein subunits in Dictyostelium.* Cell, 1989. 57(2): p. 265-75.

7. Iijima, M. and P. Devreotes, *Tumor suppressor PTEN mediates sensing of chemoattractant gradients.* Cell, 2002. 109(5): p. 599-610.

8. Funamoto, S., et al., *Spatial and temporal regulation of 3-phosphoinositides by PI 3-kinase and PTEN mediates chemotaxis.* Cell, 2002. 109(5): p. 611-23.

9. Zhou, K., et al., *A phosphatidylinositol (PI) kinase gene family in Dictyostelium discoideum: biological roles of putative mammalian p110 and yeast Vps34p PI 3-kinase homologs during growth and development.* Mol Cell Biol, 1995. 15(10): p. 5645-56.

10. Chung, C.Y., et al., *A novel, putative MEK kinase controls developmental timing and spatial patterning in Dictyostelium and is regulated by ubiquitin-mediated protein degradation.* Genes Dev, 1998. 12(22): p. 3564-78.

11. Bush, J., et al., *A role for a Rab4-like GTPase in endocytosis and in regulation of contractile vacuole structure and function in Dictyostelium discoideum.* Mol Biol Cell, 1996. 7(10): p. 1623-38.

12. Clarke, M., et al., *Dynamics of the vacuolar H(+)-ATPase in the contractile vacuole complex and the endosomal pathway of Dictyostelium cells.* J Cell Sci, 2002. 115(Pt 14): p. 2893-905.

13. Neuhaus, E.M., W. Almers, and T. Soldati, *Morphology and dynamics of the endocytic pathway in Dictyostelium discoideum.* Mol Biol Cell, 2002. 13(4): p. 1390-407.

14. Nolta, K.V., J.M. Rodriguez-Paris, and T.L. Steck, *Analysis of successive endocytic compartments isolated from Dictyostelium discoideum by magnetic fractionation.* Biochim Biophys Acta, 1994. 1224(2): p. 237-46.

15. Gerisch, G., J. Heuser, and M. Clarke, *Tubular-vesicular transformation in the contractile vacuole system of Dictyostelium.* Cell Biol Int, 2002. 26(10): p. 845-52.

16. Heuser, J., Q. Zhu, and M. Clarke, *Proton pumps populate the contractile vacuoles of Dictyostelium amoebae.* J Cell Biol, 1993. 121(6): p. 1311-27.

17. Heuser, J., *Evidence for recycling of contractile vacuole membrane during osmoregulation in Dictyostelium amoebae--a tribute to Gunther Gerisch.* Eur J Cell Biol, 2006. 85(9-10): p. 859-71.

18. Allen, R.D., *The contractile vacuole and its membrane dynamics.* Bioessays, 2000. 22(11): p. 1035-42.

19. Gabriel, D., et al., *The contractile vacuole network of Dictyostelium as a distinct organelle: its dynamics visualized by a GFP marker protein.* J Cell Sci, 1999. 112 (Pt 22): p. 3995-4005.

20. Sesaki, H., E.F. Wong, and C.H. Siu, *The cell adhesion molecule DdCAD-1 in Dictyostelium is targeted to the cell surface by a nonclassical transport pathway involving contractile vacuoles.* J Cell Biol, 1997. 138(4): p. 939-51.

21. Wilczynska, Z., et al., *Release of Ca2+ from the endoplasmic reticulum contributes to Ca2+ signaling in Dictyostelium discoideum.* Eukaryot Cell, 2005. 4(9): p. 1513-25.

22. Moniakis, J., M.B. Coukell, and A. Janiec, *Involvement of the Ca2+-ATPase PAT1*

and the contractile vacuole in calcium regulation in Dictyostelium discoideum. J Cell Sci, 1999. 112 (Pt 3): p. 405-14.

23. Malchow, D., et al., *The contractile vacuole in Ca2+-regulation in Dictyostelium: its essential function for cAMP-induced Ca2+-influx.* BMC Dev Biol, 2006. 6: p. 31.

24. Flaadt, H., E. Jaworski, and D. Malchow, *Evidence for two intracellular calcium pools in Dictyostelium: the cAMP-induced calcium influx is directed into a NBD-Cl- and 2,5-di-(tert-butyl)1,4-hydroquinone-sensitive pool.* J Cell Sci, 1993. 105 (Pt 4): p. 1131-5.

25. Beyenbach, K.W. and H. Wieczorek, *The V-type H+ ATPase: molecular structure and function, physiological roles and regulation.* J Exp Biol, 2006. 209(Pt 4): p. 577-89.

26. Dietz, K.J., et al., *Significance of the V-type ATPase for the adaptation to stressful growth conditions and its regulation on the molecular and biochemical level.* J Exp Bot, 2001. 52(363): p. 1969-80.

27. Harris, E., et al., *Rab11-like GTPase associates with and regulates the structure and function of the contractile vacuole system in dictyostelium.* J Cell Sci, 2001. 114(Pt 16): p. 3035-45.

28. Gerald, N.J., M. Siano, and A. De Lozanne, *The Dictyostelium LvsA protein is localized on the contractile vacuole and is required for osmoregulation.* Traffic, 2002. 3(1): p. 50-60.

29. Harris, E. and J. Cardelli, *RabD, a Dictyostelium Rab14-related GTPase, regulates phagocytosis and homotypic phagosome and lysosome fusion.* J Cell Sci, 2002. 115(Pt 18): p. 3703-13.

30. Wu, W.I., et al., *Structure-function analysis of the BEACH protein LvsA.* Traffic, 2004. 5(5): p. 346-55.

31. Becker, M., M. Matzner, and G. Gerisch, *Drainin required for membrane fusion of the contractile vacuole in Dictyostelium is the prototype of a protein family also represented in man.* Embo J, 1999. 18(12): p. 3305-16.

32. Bush, J., et al., *A Rab4-like GTPase in Dictyostelium discoideum colocalizes with V-H(+)-ATPases in reticular membranes of the contractile vacuole complex and in lysosomes.* J Cell Sci, 1994. 107 (Pt 10): p. 2801-12.

33. Zhu, Q. and M. Clarke, *Association of calmodulin and an unconventional myosin with the contractile vacuole complex of Dictyostelium discoideum.* J Cell Biol, 1992. 118(2): p. 347-58.

34. Doberstein, S.K., et al., *Inhibition of contractile vacuole function in vivo by antibodies against myosin-I.* Nature, 1993. 365(6449): p. 841-3.

35. Tani, T., R.D. Allen, and Y. Naitoh, *Cellular membranes that undergo cyclic changes in tension: Direct measurement of force generation by an in vitro contractile vacuole of Paramecium multimicronucleatum.* J Cell Sci, 2001. 114(Pt 4): p. 785-95.

36. Tani, T., et al., *Development of periodic tension in the contractile vacuole complex membrane of paramecium governs its membrane dynamics.* Cell Biol Int, 2002. 26(10): p. 853-60.

37. Barbosa, M.D., et al., *Identification of the homologous beige and Chediak-Higashi syndrome genes.* Nature, 1996. 382(6588): p. 262-5.

38. Introne, W., R.E. Boissy, and W.A. Gahl, *Clinical, molecular, and cell biological aspects of Chediak-Higashi syndrome.* Mol Genet Metab, 1999. 68(2): p. 283-303.

39. Spritz, R.A., *Genetic defects in Chediak-Higashi syndrome and the beige mouse.* J Clin Immunol, 1998. 18(2): p. 97-105.

40. Harris, E., et al., *Dictyostelium LvsB mutants model the lysosomal defects associated with Chediak-Higashi syndrome.* Mol Biol Cell, 2002. 13(2): p. 656-69.

41. Kwak, E., et al., *LvsA, a protein related to the mouse beige protein, is required for cytokinesis in Dictyostelium.* Mol Biol Cell, 1999. 10(12): p. 4429-39.

42. Adam-Klages, S., et al., *FAN, a novel WD-repeat protein, couples the p55 TNF-receptor to neutral sphingomyelinase.* Cell, 1996. 86(6): p. 937-47.

43. Segui, B., et al., *CD40 signals apoptosis through FAN-regulated activation of the sphingomyelin-ceramide pathway.* J Biol Chem, 1999. 274(52): p. 37251-8.

44. Segui, B., et al., *Involvement of FAN in TNF-induced apoptosis.* J Clin Invest, 2001. 108(1): p. 143-51.

45. De Lozanne, A., *The role of BEACH proteins in Dictyostelium.* Traffic, 2003. 4(1): p. 6-12.

46. Certain, S., et al., *Protein truncation test of LYST reveals heterogenous mutations in patients with Chediak-Higashi syndrome.* Blood, 2000. 95(3): p. 979-83.

47. Jogl, G., et al., *Crystal structure of the BEACH domain reveals an unusual fold and extensive association with a novel PH domain.* Embo J, 2002. 21(18): p. 4785-95.

48. Haubert, D., et al., *PtdIns(4,5)P-restricted plasma membrane localization of FAN is involved in TNF-induced actin reorganization.* Embo J, 2007.

49. Cornillon, S., et al., *Two members of the beige/CHS (BEACH) family are involved at different stages in the organization of the endocytic pathway in Dictyostelium.* J Cell Sci, 2002. 115(Pt 4): p. 737-44.

50. Charette, S.J. and P. Cosson, *A LYST/beige homolog is involved in biogenesis of Dictyostelium secretory lysosomes.* J Cell Sci, 2007. 120(Pt 14): p. 2338-43.

51. Wang, N., W.I. Wu, and A. De Lozanne, *BEACH family of proteins: phylogenetic and functional analysis of six Dictyostelium BEACH proteins.* J Cell Biochem, 2002. 86(3): p. 561-70.

52. Han, J.D., N.E. Baker, and C.S. Rubin, *Molecular characterization of a novel A kinase anchor protein from Drosophila melanogaster.* J Biol Chem, 1997. 272(42): p. 26611-9.

53. Wang, X., et al., *Neurobeachin: A protein kinase A-anchoring, beige/Chediak-higashi protein homolog implicated in neuronal membrane traffic.* J Neurosci, 2000. 20(23): p. 8551-65.

54. Zerial, M. and H. McBride, *Rab proteins as membrane organizers.* Nat Rev Mol Cell Biol, 2001. 2(2): p. 107-17.

55. Jordens, I., et al., *Rab proteins, connecting transport and vesicle fusion.* Traffic, 2005. 6(12): p. 1070-7.

56. Grosshans, B.L., D. Ortiz, and P. Novick, *Rabs and their effectors: achieving specificity in membrane traffic.* Proc Natl Acad Sci U S A, 2006. 103(32): p. 11821-7.

57. Gerald Weeks, P.G.a.R.H.I., in *Dictyostelium Genomics*, W.F.L.a.A. Kuspa, Editor. 2005, Horizon Bioscience.

58. Gotthardt, D., et al., *High-resolution dissection of phagosome maturation reveals distinct membrane trafficking phases.* Mol Biol Cell, 2002. 13(10): p. 3508-20.

59. Rupper, A., B. Grove, and J. Cardelli, *Rab7 regulates phagosome maturation in Dictyostelium.* J Cell Sci, 2001. 114(Pt 13): p. 2449-60.

60. Rupper, A., et al., *Sequential activities of phosphoinositide 3-kinase, PKB/Aakt, and Rab7 during macropinosome formation in Dictyostelium.* Mol Biol Cell, 2001. 12(9): p. 2813-24.

61. Buczynski, G., et al., *Evidence for a recycling role for Rab7 in regulating a late step in endocytosis and in retention of lysosomal enzymes in Dictyostelium discoideum.* Mol Biol Cell, 1997. 8(7): p. 1343-60.

62. Khurana, T., J.A. Brzostowski, and A.R. Kimmel, *A Rab21/LIM-only/CH-LIM complex regulates phagocytosis via both activating and inhibitory mechanisms.* Embo J, 2005. 24(13): p. 2254-64.

63. Laurent, O., et al., *In vitro reconstituted Dictyostelium discoideum early endosome fusion is regulated by Rab7 but proceeds in the absence of ATP-Mg2+ from the bulk solution.* J Biol Chem, 1998. 273(2): p. 793-9.

64. Powell, R.R. and L.A. Temesvari, *Involvement of a Rab8-like protein of Dictyostelium discoideum, Sas1, in the formation of membrane extensions, secretion and adhesion during development.* Microbiology, 2004. 150(Pt 8): p. 2513-25.

65. Pfeffer, S.R., *Rab GTPases: specifying and deciphering organelle identity and function.* Trends Cell Biol, 2001. 11(12): p. 487-91.

66. Bernards, A., *GAPs galore! A survey of putative Ras superfamily GTPase activating proteins in man and Drosophila.* Biochim Biophys Acta, 2003. 1603(2): p. 47-82.

67. Itoh, T., et al., *Screening for target Rabs of TBC (Tre-2/Bub2/Cdc16) domain-containing proteins based on their Rab-binding activity.* Genes Cells, 2006. 11(9): p. 1023-37.

68. Itoh, T. and M. Fukuda, *Identification of EPI64 as a GTPase-activating protein specific for Rab27A.* J Biol Chem, 2006. 281(42): p. 31823-31.

69. Haas, A.K., et al., *A GTPase-activating protein controls Rab5 function in endocytic trafficking.* Nat Cell Biol, 2005. 7(9): p. 887-93.

70. Knetsch, M.L., et al., *The Dictyostelium Bcr/Abr-related protein DRG regulates both Rac- and Rab-dependent pathways.* Embo J, 2001. 20(7): p. 1620-9.

71. Chung, C.Y., G. Potikyan, and R.A. Firtel, *Control of cell polarity and chemotaxis by Akt/PKB and PI3 kinase through the regulation of PAKa.* Mol Cell, 2001. 7(5): p. 937-47.

72. Goley, E.D. and M.D. Welch, *The ARP2/3 complex: an actin nucleator comes of age.* Nat Rev Mol Cell Biol, 2006. 7(10): p. 713-26.

73. Han, J.W., et al., *Role of RacC for the regulation of WASP and phosphatidylinositol 3-kinase during chemotaxis of Dictyostelium.* J Biol Chem, 2006. 281(46): p. 35224-34.

74. Myers, S.A., et al., *A Dictyostelium homologue of WASP is required for polarized F-actin assembly during chemotaxis.* Mol Biol Cell, 2005. 16(5): p. 2191-206.

75. Caracino, D., et al., *The N-terminus of Dictyostelium Scar interacts with Abi and HSPC300 and is essential for proper regulation and function.* Mol Biol Cell, 2007. 18(5): p. 1609-20.

76. Park, K.C., et al., *Rac regulation of chemotaxis and morphogenesis in Dictyostelium.* Embo J, 2004. 23(21): p. 4177-89.

77. Sasaki, A.T., et al., *Localized Ras signaling at the leading edge regulates PI3K, cell polarity, and directional cell movement.* J Cell Biol, 2004. 167(3): p. 505-18.

78. Wick, U., D. Malchow, and G. Gerisch, *Cyclic-AMP stimulated calcium influx into aggregating cells of Dictyostelium discoideum.* Cell Biol Int Rep, 1978. 2(1): p. 71-9.

79. Milne, J.L. and P.N. Devreotes, *The surface cyclic AMP receptors, cAR1, cAR2, and cAR3, promote Ca2+ influx in Dictyostelium discoideum by a G alpha 2-independent mechanism.* Mol Biol Cell, 1993. 4(3): p. 283-92.

80. Schlatterer, C., et al., *Challenge with high concentrations of cyclic AMP induces transient changes in the cytosolic free calcium concentration in Dictyostelium discoideum.* J Cell Sci, 1994. 107 (Pt 8): p. 2107-15.

81. Unterweger, N. and C. Schlatterer, *Introduction of calcium buffers into the cytosol of Dictyostelium discoideum amoebae alters cell morphology and inhibits chemotaxis.* Cell Calcium, 1995. 17(2): p. 97-110.

82. Witke, W., et al., *The Ca(2+)-binding domains in non-muscle type alpha-actinin: biochemical and genetic analysis.* J Cell Biol, 1993. 121(3): p. 599-606.

83. Yamamoto, K., et al., *Mechanism of interaction of Dictyostelium severin with actin filaments.* J Cell Biol, 1982. 95(3): p. 711-9.

84. Pikzack, C., et al., *Role of calcium-dependent actin-bundling proteins: characterization of Dictyostelium mutants lacking fimbrin and the 34-kilodalton protein.* Cell Motil Cytoskeleton, 2005. 62(4): p. 210-31.

85. Berridge, M.J., M.D. Bootman, and P. Lipp, *Calcium--a life and death signal.* Nature, 1998. 395(6703): p. 645-8.

86. Traynor, D., et al., *Ca(2+) signalling is not required for chemotaxis in Dictyostelium.* Embo J, 2000. 19(17): p. 4846-54.

87. van Haastert, P.J., I. Keizer-Gunnink, and A. Kortholt, *Essential role of*

PI3-kinase and phospholipase A2 in Dictyostelium discoideum chemotaxis. J Cell Biol, 2007. 177(5): p. 809-16.

88. Kuroki, M. and J.T. O'Flaherty, *Differential effects of a mitogen-activated protein kinase kinase inhibitor on human neutrophil responses to chemotactic factors.* Biochem Biophys Res Commun, 1997. 232(2): p. 474-7.

89. Brahmbhatt, A.A. and R.L. Klemke, *ERK and RhoA differentially regulate pseudopodia growth and retraction during chemotaxis.* J Biol Chem, 2003. 278(15): p. 13016-25.

90. Stahle, M., et al., *Mechanisms in LPA-induced tumor cell migration: critical role of phosphorylated ERK.* J Cell Sci, 2003. 116(Pt 18): p. 3835-46.

91. Mendoza, M.C., et al., *MEK1 and protein phosphatase 4 coordinate Dictyostelium development and chemotaxis.* Mol Cell Biol, 2007. 27(10): p. 3817-27.

92. Ma, H., et al., *The Dictyostelium MAP kinase kinase DdMEK1 regulates chemotaxis and is essential for chemoattractant-mediated activation of guanylyl cyclase.* Embo J, 1997. 16(14): p. 4317-32.

93. Sobko, A., H. Ma, and R.A. Firtel, *Regulated SUMOylation and ubiquitination of DdMEK1 is required for proper chemotaxis.* Dev Cell, 2002. 2(6): p. 745-56.

94. Faix, J., et al., *A rapid and efficient method to generate multiple gene disruptions in Dictyostelium discoideum using a single selectable marker and the Cre-loxP system.* Nucleic Acids Res, 2004. 32(19): p. e143.

95. Lee, S., et al., *TOR complex 2 integrates cell movement during chemotaxis and signal relay in Dictyostelium.* Mol Biol Cell, 2005. 16(10): p. 4572-83.

96. Steimle, P.A., et al., *Recruitment of a myosin heavy chain kinase to actin-rich protrusions in Dictyostelium.* Curr Biol, 2001. 11(9): p. 708-13.

97. Funamoto, S., et al., *Role of phosphatidylinositol 3' kinase and a downstream pleckstrin homology domain-containing protein in controlling chemotaxis in dictyostelium.* J Cell Biol, 2001. 153(4): p. 795-810.

98. Chang, L. and M. Karin, *Mammalian MAP kinase signalling cascades.* Nature, 2001. 410(6824): p. 37-40.

99. Bradham, C. and D.R. McClay, *p38 MAPK in development and cancer.* Cell Cycle, 2006. 5(8): p. 824-8.

100. Krens, S.F., H.P. Spaink, and B.E. Snaar-Jagalska, *Functions of the MAPK family in vertebrate-development.* FEBS Lett, 2006. 580(21): p. 4984-90.

101. Gaskins, C., M. Maeda, and R.A. Firtel, *Identification and functional analysis of a developmentally regulated extracellular signal-regulated kinase gene in Dictyostelium discoideum.* Mol Cell Biol, 1994. 14(10): p. 6996-7012.

102. Mendoza, M.C., et al., *Loss of SMEK, a novel, conserved protein, suppresses MEK1 null cell polarity, chemotaxis, and gene expression defects.* Mol Cell Biol, 2005. 25(17): p. 7839-53.

103. Jacobs, D., et al., *Multiple docking sites on substrate proteins form a modular system that mediates recognition by ERK MAP kinase.* Genes Dev, 1999. 13(2): p. 163-75.

104. Albert, S., E. Will, and D. Gallwitz, *Identification of the catalytic domains and their functionally critical arginine residues of two yeast GTPase-activating proteins specific for Ypt/Rab transport GTPases.* Embo J, 1999. 18(19): p. 5216-25.

105. Rak, A., et al., *Crystal structure of the GAP domain of Gyp1p: first insights into interaction with Ypt/Rab proteins.* Embo J, 2000. 19(19): p. 5105-13.

106. Pan, X., et al., *TBC-domain GAPs for Rab GTPases accelerate GTP hydrolysis by a dual-finger mechanism.* Nature, 2006. 442(7100): p. 303-6.

107. Schneider, N., et al., *Golvesin-GFP fusions as distinct markers for Golgi and post-Golgi vesicles in Dictyostelium cells.* Biol Cell, 2000. 92(7): p. 495-511.

108. Kriebel, P.W., V.A. Barr, and C.A. Parent, *Adenylyl cyclase localization regulates streaming during chemotaxis.* Cell, 2003. 112(4): p. 549-60.

109. Heo, W.D., et al., *PI(3,4,5)P3 and PI(4,5)P2 lipids target proteins with polybasic*

clusters to the plasma membrane. Science, 2006. 314(5804): p. 1458-61.

110. Lechner, E., et al., *F-box proteins everywhere.* Curr Opin Plant Biol, 2006. 9(6): p. 631-8.

111. Bos, J.L., H. Rehmann, and A. Wittinghofer, *GEFs and GAPs: critical elements in the control of small G proteins.* Cell, 2007. 129(5): p. 865-77.

112. Martinu, L., et al., *The TBC (Tre-2/Bub2/Cdc16) domain protein TRE17 regulates plasma membrane-endosomal trafficking through activation of Arf6.* Mol Cell Biol, 2004. 24(22): p. 9752-62.

113. Hattula, K., et al., *Characterization of the Rab8-specific membrane traffic route linked to protrusion formation.* J Cell Sci, 2006. 119(Pt 23): p. 4866-77.

114. Kipreos, E.T. and M. Pagano, *The F-box protein family.* Genome Biol, 2000. 1(5): p. REVIEWS3002.

115. Russell, I.D., A.S. Grancell, and P.K. Sorger, *The unstable F-box protein p58-Ctf13 forms the structural core of the CBF3 kinetochore complex.* J Cell Biol, 1999. 145(5): p. 933-50.

116. Kondo-Okamoto, N., et al., *The novel F-box protein Mfb1p regulates mitochondrial connectivity and exhibits asymmetric localization in yeast.* Mol Biol Cell, 2006. 17(9): p. 3756-67.

117. Galan, J.M., et al., *Skp1p and the F-box protein Rcy1p form a non-SCF complex involved in recycling of the SNARE Snc1p in yeast.* Mol Cell Biol, 2001. 21(9): p. 3105-17.

118. Kaplan, K.B., A.A. Hyman, and P.K. Sorger, *Regulating the yeast kinetochore by ubiquitin-dependent degradation and Skp1p-mediated phosphorylation.* Cell, 1997. 91(4): p. 491-500.

119. Huber, L.A., et al., *Rab8, a small GTPase involved in vesicular traffic between the TGN and the basolateral plasma membrane.* J Cell Biol, 1993. 123(1): p. 35-45.

120. Chen, W., et al., *Rab11 is required for trans-golgi network-to-plasma membrane transport and a preferential target for GDP dissociation inhibitor.* Mol Biol Cell,

1998. 9(11): p. 3241-57.

121. Junutula, J.R., et al., *Rab14 is involved in membrane trafficking between the Golgi complex and endosomes.* Mol Biol Cell, 2004. 15(5): p. 2218-29.

122. Proikas-Cezanne, T., et al., *Rab14 is part of the early endosomal clathrin-coated TGN microdomain.* FEBS Lett, 2006. 580(22): p. 5241-6.

123. Wang, J.W., et al., *Deregulated expression of LRBA facilitates cancer cell growth.* Oncogene, 2004. 23(23): p. 4089-97.

124. Castermans, D., et al., *The neurobeachin gene is disrupted by a translocation in a patient with idiopathic autism.* J Med Genet, 2003. 40(5): p. 352-6.

125. Stavrou, I. and T.J. O'Halloran, *The monomeric clathrin assembly protein, AP180, regulates contractile vacuole size in Dictyostelium discoideum.* Mol Biol Cell, 2006. 17(12): p. 5381-9.

126. Lefkir, Y., et al., *The AP-1 clathrin-adaptor is required for lysosomal enzymes sorting and biogenesis of the contractile vacuole complex in Dictyostelium cells.* Mol Biol Cell, 2003. 14(5): p. 1835-51.

127. O'Halloran, T.J. and R.G. Anderson, *Clathrin heavy chain is required for pinocytosis, the presence of large vacuoles, and development in Dictyostelium.* J Cell Biol, 1992. 118(6): p. 1371-7.

128. Khodosh, R., et al., *Bchs, a BEACH domain protein, antagonizes Rab11 in synapse morphogenesis and other developmental events.* Development, 2006. 133(23): p. 4655-65.

129. Simonsen, A., et al., *Genetic modifiers of the Drosophila blue cheese gene link defects in lysosomal transport with decreased life span and altered ubiquitinated-protein profiles.* Genetics, 2007. 176(2): p. 1283-97.

130. Yoshida, K. and K. Inouye, *Myosin II-dependent cylindrical protrusions induced by quinine in Dictyostelium: antagonizing effects of actin polymerization at the leading edge.* J Cell Sci, 2001. 114(Pt 11): p. 2155-65.

131. Yoshida, K., et al., *A voltage- and K+-dependent K+ channel from a membrane*

fraction enriched in contractile vacuole of Dictyostelium discoideum. Biochim Biophys Acta, 1997. 1325(2): p. 178-88.

132. Rooney, E.K. and J.D. Gross, *ATP-driven Ca2+/H+ antiport in acid vesicles from Dictyostelium.* Proc Natl Acad Sci U S A, 1992. 89(17): p. 8025-9.

133. Clark, R.A. and H.R. Kimball, *Defective granulocyte chemotaxis in the Chediak-Higashi syndrome.* J Clin Invest, 1971. 50(12): p. 2645-52.

134. Korzynska, A., *Neutrophils movement in vitro.* Ann N Y Acad Sci, 2002. 972: p. 139-43.

135. De la Roche, M.A., et al., *Signaling pathways regulating Dictyostelium myosin II.* J Muscle Res Cell Motil, 2002. 23(7-8): p. 703-18.

136. Kollmar, M., *Thirteen is enough: the myosins of Dictyostelium discoideum and their light chains.* BMC Genomics, 2006. 7: p. 183.

137. Jones, M.C., P.T. Caswell, and J.C. Norman, *Endocytic recycling pathways: emerging regulators of cell migration.* Curr Opin Cell Biol, 2006. 18(5): p. 549-57.

138. Shirane, M. and K.I. Nakayama, *Protrudin induces neurite formation by directional membrane trafficking.* Science, 2006. 314(5800): p. 818-21.